coatings

MDPI

Review

Nanomaterials for Anti-Infection in Orthopedic Implants: A Review

Junhao Sui [1,†], Yijin Hou [2,†], Mengchen Chen [1,†], Zhong Zheng [1], Xiangyu Meng [1], Lu Liu [1], Shicheng Huo [3,*], Shu Liu [4,*] and Hao Zhang [1,*]

[1] Department of Orthopedics, Changhai Hospital, Navy Medical University, Shanghai 200433, China
[2] School of Medical Instrument and Food Engineering, University of Shanghai for Science and Technology, Shanghai 200093, China
[3] Department of Orthopedic Surgery, Spine Center, Changzheng Hospital, Navy Medical University, Shanghai 200003, China
[4] Department of Spine Surgery, Changhai Hospital, Navy Medical University, Shanghai 200433, China
* Correspondence: waznxyz@126.com (S.H.); acoliushu@163.com (S.L.); zhanghsmmu@126.com (H.Z.)
† These authors contributed equally to this work.

Abstract: Postoperative implant infection is a severe complication in orthopedic surgery, often leading to implant failure. Current treatment strategies mainly rely on systemic antibiotic therapies, despite contributing to increasing bacterial resistance. In recent years, nanomaterials have gained attention for their potential in anti-infection methods. They exhibit more substantial bactericidal effects and lower drug resistance than conventional antimicrobial agents. Nanomaterials also possess multiple bactericidal mechanisms, such as physico-mechanical interactions. Additionally, they can serve as carriers for localized antimicrobial delivery. This review explores recent applications of nanomaterials with different morphologies in post-orthopedic surgery infections and categorizes their bactericidal mechanisms.

Keywords: nanomaterials; antimicrobial; orthopedic implants

Citation: Sui, J.; Hou, Y.; Chen, M.; Zheng, Z.; Meng, X.; Liu, L.; Huo, S.; Liu, S.; Zhang, H. Nanomaterials for Anti-Infection in Orthopedic Implants: A Review. *Coatings* **2024**, *14*, 254. https://doi.org/10.3390/coatings14030254

Academic Editor: Eugenio Velasco-Ortega

Received: 16 January 2024
Revised: 15 February 2024
Accepted: 19 February 2024
Published: 21 February 2024

1. Introduction

Orthopedic-implant-associated infections are severe complications following orthopedic surgery caused by bacterial colonization and biofilm formation. These infections can lead to chronic microbial infection, tissue necrosis, inflammation, systemic infections, multiple organ failure, and death [1]. Biofilms are complex communities of bacterial cells that form on the surfaces of inserted biomaterials or periprosthetic tissues. They create physical and chemical barriers around the implants, making them resistant to antibiotics and the local immune system [2–5]. Biofilm formation is influenced by the surface's physical properties and chemical composition, involving the migration and adhesion of bacteria to the implant surface [6]. Moreover, the overuse and misuse of antibiotics have significantly contributed to the rise in antibiotic resistance [7,8]. Bacterial infections have emerged as a clinically significant contributor to health loss, now the second leading cause of mortality worldwide [9]. In 2019, three infectious syndromes accounted for over one million deaths each, collectively representing over 75 percent of fatalities caused by bacterial infections. It is estimated that around 0.7 million deaths occur annually due to drug-resistant bacterial infections [10]. According to the World Health Organization, infections caused by resistant bacteria are projected to result in 10 million deaths worldwide annually [11]. The annual cost of antibiotic-resistant infections in the United States is estimated to be between USD 55 and USD 70 billion. In Europe, the economic cost of multidrug-resistant (MDR) infections is more than EUR 1.5 billion per year [12,13]. Advanced nanostructured materials have been utilized to address this issue, and show promising applications in dental and orthopedic implants due to their unique antimicrobial mechanisms.

According to statistics, about 80% of medical infections come from the biofilm growth of pathogens. Currently, most implant antibacterial research focuses on killing microorganisms in the biofilm on the surface of the implant. Surface modification is a promising strategy to inhibit biofilm formation on the surface of implants and kill surface microorganisms. In clinical work, the surface of implants with micrometer topography features increases the contact area between cells and the surface due to the size being similar to that of prokaryotic cells, which is conducive to cell attachment. Compared with micron surface, nanoscale surface showed excellent antibacterial properties. Recently, growing research has focused on fabricating anti-biofouling structures and anti-adhesive surfaces for implants through surface modifications of nanomaterials. Feng et al. [14] demonstrated the effectiveness of anodic nanoporous surfaces in reducing bacterial attachment through the electrostatic repulsion between bacteria and these surfaces. Nanomaterials, such as gold, nickel, and nanoimprinted polymers, exhibit interparticle electrostatic and steric repulsion, effectively preventing microbial colonization on surfaces by reducing bacterial adhesion [15–18]. A new strategy for antibacterial surfaces and to reduce antibiotic usage has been reported, which involves utilizing the surface coating to achieve 'release killing', or 'contact inhibition', by loading antibiotics into a superhydrophilic coating.

Surface coating orthopedic implants with nanomaterials containing metal nanoparticles (NPs) or nanopolymers holds great promise for revolutionizing the antibacterial properties of metallic implants. A variety of mechanisms have been extensively studied, and several of them are now well understood. Bactericidal mechanisms through surface contact are usually divided into two categories: the stretching and rupture of bacterial cells induced by nanopillars of various sizes and shapes, and the cleavage effect of bacterial cell membranes caused by the sharp edges of nanocoatings. Previously, bacterial cells adhered to nanostructured surfaces via the physical interaction between the surface and bacteria. Furthermore, studies have shown that the release of metal ions, the generation of reactive oxygen species (ROS), and nanostructure effects can effectively inhibit or kill bacteria [19–21]. Furthermore, antibiotics can be encapsulated within hollow NPs or attached to the side chains of polymeric NPs. Subsequently, these NPs can permeate the cell wall and disrupt the fundamental functions of the bacteria [22,23]. Two-step local antibiotic delivery, consisting of an initial burst release followed by a subsequent slow release over a long duration, achieves an early, high, and local concentration of antibiotics. This approach effectively minimizes the adverse effects commonly associated with the systemic administration of high-dose antibiotics [24–26]. In the field of orthopedic implants, the use of nanoscale materials in surface coatings has become increasingly prevalent due to advancements in nanotechnology. Various bactericidal nanopatterns enable different types of substrate surfaces, including metals and polymers, to possess microbicidal properties [27]. Nevertheless, the precise mechanisms underlying the impact of nanopatterns on bacterial cell lysis remain unclear and warrant further investigation.

Recently, there has been rapid progress in the fungicidal applications of nanomaterials for antimicrobial release and their direct bactericidal effects, providing new approaches to enhance the antibacterial properties of current orthopedic implants. The objective of this study was to review previous research on preventing bacterial adhesion and colonization on nanomaterial surfaces, promoting the application of nanomaterials in the field of orthopedic infections (Table 1).

2. Antimicrobial Agents Loaded in Nanocontainers

Sterilization can be achieved using either the 'contact inhibition' or 'release killing' model by incorporating antimicrobials into the surface coating of implants [28,29]. Encapsulated antibiotics within NPs can penetrate the bacterial cell wall, ultimately disrupting critical bacterial functions [22]. Following implant placement during orthopedic surgery, the initial phase is characterized by the undesired adhesion of proteins due to infection and local inflammation. The acute inflammatory response, caused by the nonspecific adsorption of proteins, typically results in the failure of internal implants [30]. Therefore, the successful

development of superhydrophilic nonfouling coatings is deemed crucial in determining the effectiveness of orthopedic implants in preventing infections [31]. Based on current knowledge, catechol-modified coatings are effective as functional carriers for antibiotics through hydrophobic and π-π interactions [32,33]. Superhydrophilic coatings consisting of stacked NPs were fabricated by uniformly depositing polydopamine (PDA) NPs onto the surface to create a micro/nano topology. Norfloxacin (NOR) and cephalexin (CEP) were then embedded within the coating via π-π interactions and hydrophobic forces [34]. The antibacterial experiments demonstrated that the antibiotic-loaded superhydrophilic coatings (PDA/NOR and PDA/CEP) exhibited effective long-term antibacterial properties. The novel anti-infective coating, incorporating a synergistic model, displayed remarkable inhibition of nonspecific protein adhesion by leveraging the superhydrophilic property. This property synergistically enhanced the antimicrobial activity when combined with antibiotics. Overall, the simultaneous integration of nonfouling surfaces and antibiotics holds great potential and is an appealing direction to explore.

Outdated scaffolds have significant disadvantages, such as a lack of ability to effectively inhibit bacterial infections at sites of bone fractures or defects. To address this issue, Cai et al. [35] fabricated a novel injectable gel with a nanoporous and microporous structure that facilitates molecule transfer and tissue infiltration based on the assembly of chitosan microspheres (Figure 1). Berberine (Bbr) was loaded into negatively charged O-carboxymethyl chitosan microspheres (CMCSM) through swollen encapsulation and physical adsorption, with minimal alteration to their electric charges. This loading method enables the controlled release of drugs or proteins, effectively prolonging their biological effects. Berberine chloride (Bbr), a water-soluble isoquinoline alkaloid, exhibits enhanced release and transfer capabilities between microsphere assemblies due to its biological molecular properties and the presence of nanopores. The results demonstrated that the Bbr/CMCSM microspheres group exhibited significant antibacterial activity against *Staphylococcus aureus* (*S. aureus*).

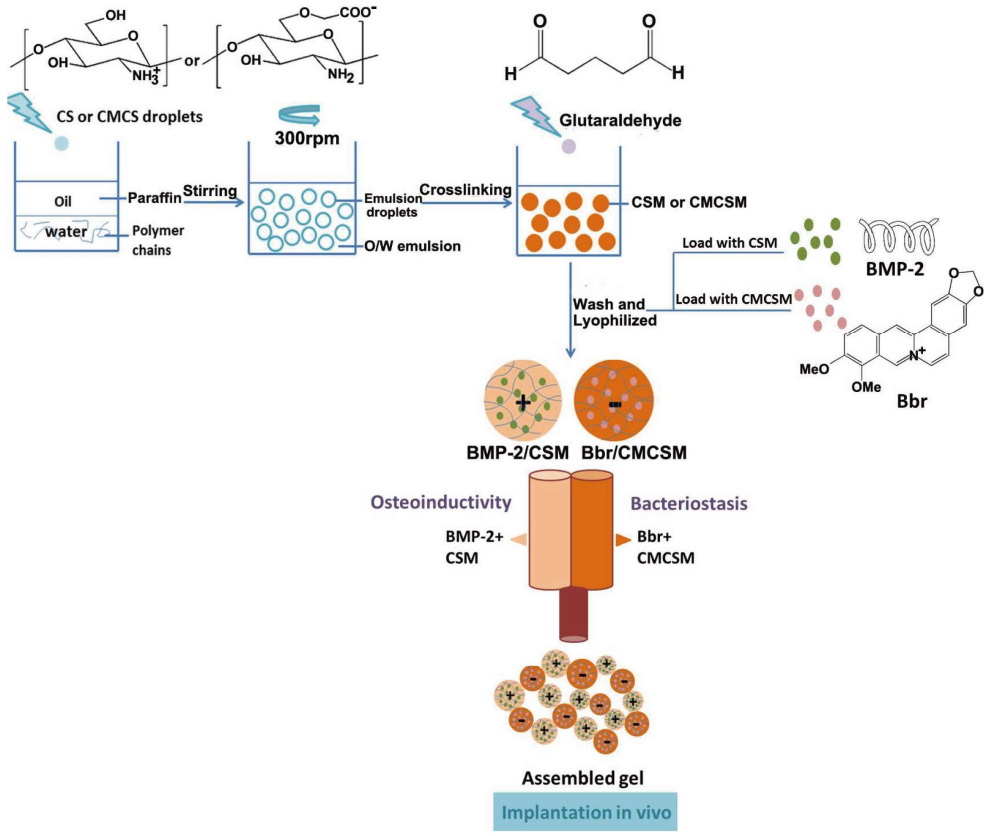

Figure 1. The assembly of oppositely charged microspheres loaded with Bbr and BMP-2 into a gel. Reprinted with permission from Ref. [35]. Copyright 2018 American Chemical Society.

Porous scaffolds are typically developed for repairing bone defects and anti-infection because of their excellent mechanical properties and biomimetic hierarchical structures. Most antimicrobial agents are physically fixed to the implant surface to protect them from contamination. However, this fixation method does not provide a long-lasting release of the agents. Han et al. [36] assembled layer-by-layer (LbL) films with nanoporous structures on Ti scaffolds by the sequential assembling of chitosan- (cationic-)coated BSA nanoparticles (CBSA-NPs) and negatively charged oxide sodium alginate (anionic) (OSA) on the scaffolds. Vancomycin (VAN) was pre-grafted onto the OSA chains through the reaction between the amino group of VAN and the aldehyde group of OSA. In vitro antibacterial tests demonstrated that the continuous release of VAN from LbL films, that were assembled on Ti scaffolds, exhibited excellent antimicrobial properties. Similarly, Yu et al. [37] developed a controlled and sustained release system loaded with vancomycin on poly(lactic-co-glycolic acid) microspheres for topical antimicrobial therapy against *S. aureus* and *MRSA*.

The porous nature of titanium nanotubes (Ti-NT) has been extensively studied, and they have been considered as nanoreservoirs for local drug delivery. However, it is difficult to control the sudden release of high drug dosage and achieve sustained drug release from nanotubes. He et al. [38] revealed the effective antibacterial potency of polydopamine (PDA) and hyaluronic acid- (Hya-)modified Ti-NT by immobilizing pDA and Hya on the VAN-loaded Ti-NT surface, employing an alternate deposition technique. In recent years, the concept of a nano-in-micro composite has been proposed as a new type of nanocomposite. It serves as a sustained drug delivery platform that incorporates the drug-loading capability of nanotubes with electrospinning technology [39,40]. Using the electrospinning technique, a nano–micro composite fiber membrane with sustained drug delivery was developed by embedding metronidazole- (MNA-)loaded clay nanotubes into electrospun microfibers. [41]. Compared to traditional drug delivery systems, the nano–micro composite membranes exhibit a minor initial drug burst release and provide sustained release of metronidazole for up to four weeks. This prolonged release effectively inhibits bacteria from surviving the initial burst during the high-incidence period of infection and inflammation. The sustained release of metronidazole from the halloysite clay nanotubes is crucial in reducing postoperative infections, particularly those caused by anaerobic bacteria. Hence, this concept offers several advantages over traditional drug delivery systems, including localized treatment and reduced toxicity. Golda-Cepa et al. devised a controlled drug delivery system by leveraging the synergistic effect of nanotopography and surface group modification of parylene C through oxygen plasma, which could effectively regulate the release of local antibiotics from the implant surface [42].

Mesoporous silica nanoparticles (MSNs) have gained significant attention as a drug-delivery carrier system due to their exceptional biocompatibility, ultrahigh specific surface area, large pore diameters, ease of surface modification, and uniform pore structures [43,44]. However, while MSNs loaded with antimicrobials can offer sustained local drug release, they often lack the ability to specifically target bone infection sites, resulting in suboptimal therapeutic outcomes. Peptide D_6, known for its effective bone-targeted drug delivery, can functionalize the surface of MSNs covalently grafted with Peptide $UBI_{29–41}$, which is a commonly used bacteria-targeted agent [45–47]. Bone-and-bacteria dual-targeted MSNs were developed to enable targeted delivery of vancomycin to the bone infection site, improving the therapeutic efficacy for orthopedic-implant-related infection (Figure 2) [48]. In another study, levofloxacin- (Lev-)loaded MSNs combined with nano-hydroxyapatite (n-HA) and polyurethane (PU) were utilized to construct a novel biodegradable composite scaffold, which can enhance osteogenesis and significantly inhibit the growth of both *E. coli* and *S. aureus* [49].

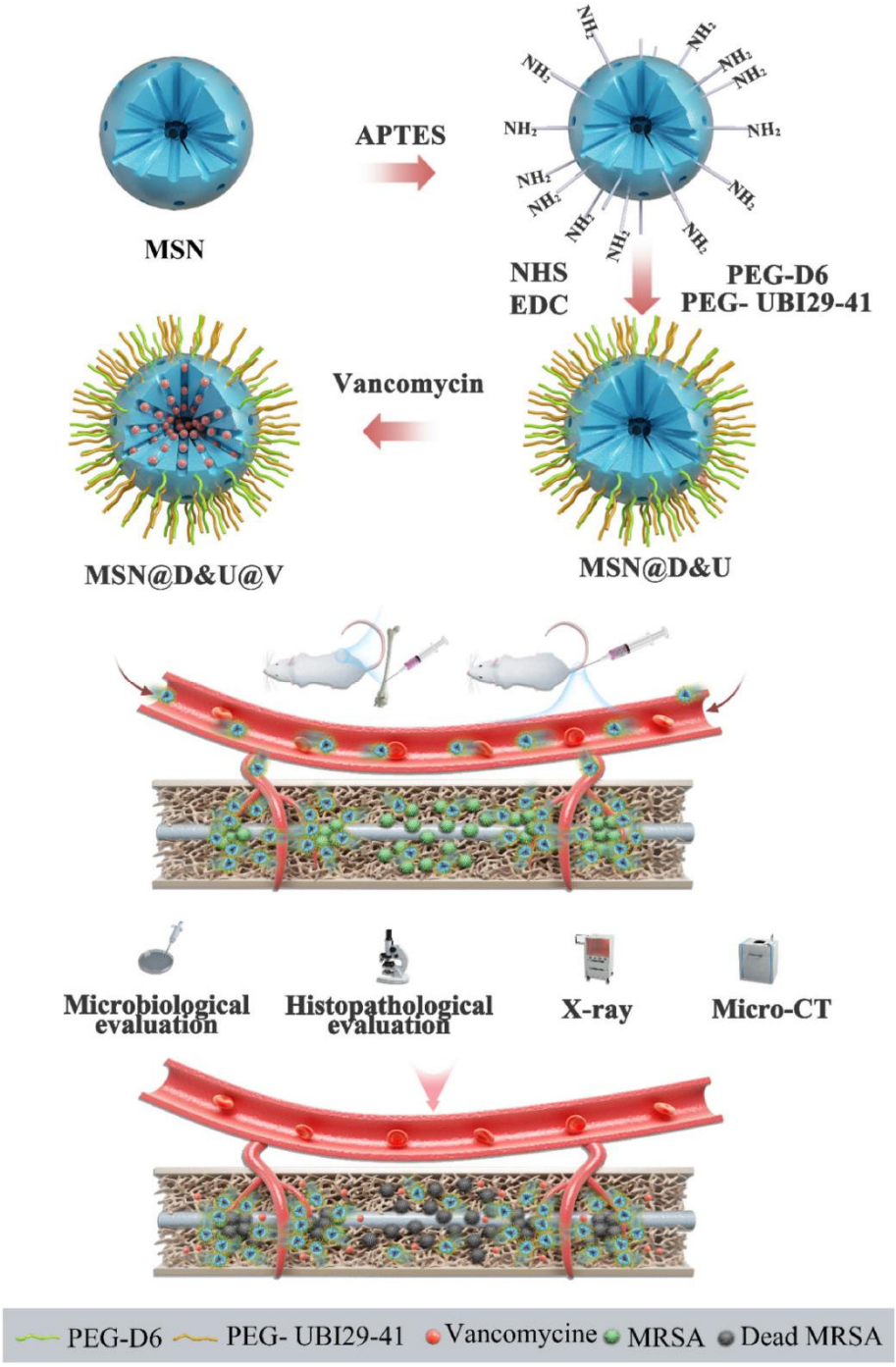

Figure 2. Synthesis of mesoporous silica nanoparticles (MSNs) with dual properties of bone-targeting and bacteria-targeting, and study of their antibacterial activity in vitro and in vivo. Reprinted with permission from ELSEVIER. This is an open access article.

Electrospinning technology is an attractive alternative to loading various drugs into nanofibers with controlled release capability [50]. MNA and nano-hydroxyapatite- (n-HA-)loaded core-shell nanofibers have been fabricated using coaxial electrospinning. The MNA is loaded in the nanofiber core to achieve sustained and slow release, thereby reducing drug toxicity [51]. Compared to 80% MNA released on the first day for nanofibers without core-shell structure, a PCL/nHA core-gelatin/MNA shell reduces the initial burst release to approximately 55% due to its core-shell structure. There are distinct bacterial inhibition zones surrounding the membrane of the bacterial nanofibers with a core-shell structure.

3. Metal Nanoparticles

The excellent antibacterial properties of different metal/metal-oxide NPs have been extensively reported in various fields, including nanomedicine, industries, and cosmetics [52–54]. The nanosurface properties of materials can be manipulated to regulate biological functions, such as antibacterial activity, cell adhesion, and proliferation. In recent years, multiple studies have demonstrated the use of nanotechnology in constructing nanostructured surfaces to manipulate and modify the antimicrobial properties of orthopedic implants [55]. Metal-based antibacterial surfaces on implants have long been recognized for killing bacteria by releasing metallic ions [56]. However, many studies have revealed that metal/metal-oxide NPs exhibit higher antibacterial activity and lower cytotoxicity [57,58].

Although the precise antimicrobial mechanism requires further investigation and discussion, several mechanisms proposed in the literature are as follows: disruption of bacterial cell membranes, leading to cell death [59]; liberation of antimicrobial ions, inducing oxidative stress and ROS formation [60–62]; inhibition of bacterial cell wall synthesis and DNA replication through interaction with the functional group of proteins [63–65]; inhibition of cellular energy metabolism [66]; and increased permeability of the bacterial cell membrane [67], which may also contribute to antimicrobial activity.

Silver, zinc, and copper NPs have significant potential as antibacterial agents, and thus they are commonly applied as a surface modification of implants [68–70]. Silver NPs have been widely utilized as antibacterial agents in orthopedic surgery for a long time because of their broad-spectrum antibacterial activity against various bacteria and fungi. A conceptual strategy called 'prophylaxis/fighting–repair' was proposed for multifunctional anti-infection and bone repair [71]. In this study, a mass of micro/nanoscale pores drastically increased the total surface area of scaffolds and, thus, the capacity for immobilizing silver nanoparticles (AgNPs). By combining highly porous hydrogels with AgNPs, Antezana et al. developed a novel biomaterial with a long-term antibacterial effect to achieve controlled and delayed release of NPs, improving the mechanical properties of the hydrogel [72]. The antimicrobial effect of nanosilver from micro/nanoporous surfaces is attributed to the sustained release of ionic silver ions and the generation of reactive oxygen species (ROS). The tight binding between ionic silver and the bacterial membrane via Ag-S bonds or electrostatic attraction induces the formation of nanopores on the membrane, leading to membrane damage [73]. The antibacterial properties of AgNPs are influenced by particle sizes. In general, smaller AgNPs exhibit better antibacterial activity [74]. Meanwhile, a more substantial antibacterial property results in a smaller required dose and lower biotoxicity. Xue et al. combined 3D-printing technology and surface-nanocoating modification to develop a novel implantation system capable of regulating the release of AgNPs from the membrane [75]. AgNPs have the potential to adhere to the bacterial surface and interfere with the permeability and respiratory function of bacterial cells. Furthermore, AgNPs impact the bacterial membrane and can penetrate the bacterial interior [76]. AgNPs smaller than 10 nm can attach to the surface of bacterial cell walls, and 5 ± 2 nm of these particles can penetrate the bacterial interior [77]. AgNPs penetrate the membrane and destroy protein, thereby deactivating crucial microbial enzymes and killing bacteria [78]. They can also generate ROS, specifically superoxide radicals, which subsequently influence cellular activities, further destroying the cell structure and ultimately causing bacterial death [79,80]. Moreover, additional mechanisms involving charge transfer between silver and bacteria have been discovered. These interactions disrupt the extracellular electron transfer process, which is essential for bacterial energy production, ultimately leading to their demise [81]. These mechanisms create sustained antibacterial microenvironments around orthopedic implants, preventing bacterial adhesion on the implant surface and biofilm formation for extended periods. Moreover, these mechanisms effectively disrupt existing biofilms.

Copper has also been proven to be involved in ROS generation, and the hydroxyl radical generated from copper ions is highly toxic to bacteria [82]. Furthermore, the bactericidal mechanism of copper may involve the substitution of iron in crucial enzymes or

the blockade of zinc-binding sites on bacterial proteins [83]. Researchers fabricated hybrid copper-/silver-based polydopamine nanoparticles (Cu/Ag-PDA-NPs) by chelating copper to the shell of dopamine nanoparticles (PDA-NPs) and synthesizing sonochemically with Ag-PDA-NPs. The released copper ions from these NPs demonstrated strong antibacterial effects and effectively inhibited biofilm formation. [84]. Copper nanoparticles (CuNPs) exhibit more potent antimicrobial activity than AgNPs against existing *P. aeruginosa* biofilms, although silver ions have a stronger bactericidal ability than copper ions. However, both metal NPs exhibit equal activity against *S. mutans* biofilms. Compared to silver ions, copper ions exhibit enhanced penetration into the exopolymeric matrix. Other studies have shown that copper ions can effectively impede the formation of bacterial biofilms by inhibiting the expression of proteins that dominate biofilm formation, even without killing the bacteria [85]. CuNPs have been shown to efficiently prevent bacterial biofilm formation and eradicate existing biofilms that are typically resistant to traditional antibiotic treatment [86,87].

Li et al. developed micro–nano materials from bioactive glass (BG) with the dual biological properties of osteogenesis promotion and biocompatibility, incorporating zinc nanoparticles (ZnNPs) for osteogenesis and control of infection and inflammation [88]. The incorporation of zinc (Zn) amplified the antibacterial ability of Zn-doped bioactive glass (BG), thereby demonstrating superior antibacterial properties relative to the other groups. In addition, zinc ions were shown to participate in homeostasis and angiogenesis in this study. The antibacterial action of ZnNPs is influenced by various factors, including their attachment to the cell membrane, accumulation within cells, and intracellular ROS generation [89]. The results are consistent with previous studies, which indicated that ZnNPs induce oxidative stress in bacterial cells and disrupt the cell membrane and DNA, eventually resulting in bacterial death [90]. The production of ROS is mediated by the interaction between zinc ions and the thiol group of bacterial respiratory enzymes [91,92].

Gold nanoparticles (AuNPs) showed potent antibacterial activity against *E. coli* and other bacteria [93]. Moreover, AuNPs without any toxic effect on epithelial and fibroblast cells are becoming increasingly favored [94,95]. A porous nano-gold/polyurethane scaffold was developed, in which AuNPs and polyurethane were mixed. The polymer matrix and porous samples were obtained by incorporating sodium chloride into the mixture [96]. A small quantity of AuNPs resulted in a remarkable 99.99% inhibition rate against both *S. epidermidis* and *Klebsiella* spp. Most antibacterial nanomaterials cause bacterial death by destructing and penetrating bacterial walls and membranes with metal ions, generating ROS, forming condensed DNA, and inhibiting ATP synthesis [97,98]. However, AuNPs involved in sterilization have been proven not to induce any ROS-related processes [97]. AuNPs primarily exert their antibacterial effect through two mechanisms: inhibiting the activities of ATP synthase to slow down metabolism, and reducing the binding of ribosomal subunits to tRNA, disrupting biological processes. The investigators also discovered a noticeable increase in ions released from sea-urchin-shaped AuNPs when compared to nanospheres or nanorods, thereby increasing the antimicrobial activity associated with a larger exposed surface.

With the widespread application of metal/metal oxide nanostructured coating in recent years, the cytotoxicity associated with metal ions has been increasingly recognized. AgNPs have been extensively utilized in orthopedic implants for their powerful antibacterial properties. However, recent research has demonstrated that, at high concentrations, they had a cytotoxic effect on healthy cells such as hepatocytes [99]. Moreover, it is widely recognized that elevated levels of CuNPs can induce cytotoxic effects [100]. The toxicity of copper is strongly influenced by its speciation. Cupric ions have been identified as the most toxic form of copper, in which Cu (II) (cupric ion) can be used as an antibacterial agent and also cause tissue oxidative stress and cell apoptosis [101]. The toxicity of ZnNPs, determined by diverse physicochemical characteristics of NPs and photocatalytic ROS production, is affected by NP formulation, size, and surface structure [102]. There is already evidence indicating that high concentrations of ZnNPs cause adverse effects on organism

development, resulting in a changed expression of oxidation-related genes, including the down-regulated expression of antioxidant protein (Bcl-2, Nqo1, and Gstp2) genes and up-regulated transcript levels of uncoupling protein 2 (Ucp-2) [103]. The bactericidal mechanism of the ROS independence of AuNPs can partially account for the low toxicity of AuNPs towards mammalian cells. The toxicity of AuNPs generally depends on their particle size, surface charge, and hydrophobicity [104]. AuNPs smaller than 15 nm can pass through the skin and intestine [105]. Animal studies have shown that medium-sized AuNPs (8–37 nm) induce lethality in mice, resulting in weight loss, decreased appetite, and shortened half-life [106]. In addition, it has been observed that AuNPs with amphiphilic chains can circulate in the blood for a longer time, owing to the attenuation of phagocytosis in the liver. Furthermore, the prolonged presence of negatively charged AuNPs adversely affects the liver and spleen [107].

4. Metal Oxide Nanoparticles

Metal oxide NPs have exhibited excellent antimicrobial activity. Zinc oxide nanoparticles (ZnO-NPs), which possess antibacterial properties and facilitate wound healing, have been loaded onto electrospinning fibers to prepare composite nanomaterials with the inhibition of *S. aureus* and *E. coli* [70]. In this study, ZnONPs were synthesized by a sustainable process using the Ilex paraguariensis leaves, which can yield low-toxicity NPs. In addition, studies have shown that the cytotoxicity of ZnO-NPs can be mitigated by their incorporation with fibers [108]. Like metal NPs, the antimicrobial mechanisms of metal oxide NPs involve nanoparticle internalization, membranolysis, and ROS generation [109]. In other studies, composite materials like chitosan and hydrogels modified with ZnO-NPs have shown remarkable antibacterial effects against multiple bacteria, including Gram-positive and Gram-negative bacteria [110–113]. The investigators found that zinc ions released by ZnO-NPs bind to negatively charged bacterial cell membranes, leading to their lysis. The toxicity of ZnO-NPs depends on their concentration, drug delivery route, exposure duration, and nanoparticle size [114]. ZnO-NPs at concentrations above 50 μg/mL show toxicity to the HGF-1 human gingival fibroblast cells [115]. However, ZnO-NP exhibits potential genotoxicity to human epidermal cells even at concentrations below 1 μg/mL [116].

Karuppannan et al. prepared antibacterial nanofiber materials by loading copper oxide NPs onto electrospun nanofibers based on polycaprolactone and gelatin [117]. In vitro antimicrobial experiments showed that the nanofibers exhibit robust antibacterial ability against *S. aureus*, *E. coli*, and *P. aeruginosa*. The antibacterial mechanism of CuO-NPs has been demonstrated to involve the generation of ROS through Fenton-like and Haber–Weiss reactions, which oxidize the cell membrane and subsequently destroy the bacterial cell. CuO-NPs show a higher cytotoxic potential than other metal oxide NPs [118]. Moreover, compared to other sizes, the toxicity of CuO-NPs at the nanoscale was observed to increase. High concentrations of CuO-NPs cause cytotoxicity, which results from the released cupric ions [119]. CuO-NPs loaded with a concentration higher than 1% showed cytotoxicity against NIH3T3 cells [120]. CuO-NPs exhibit genotoxicity and disrupt the HaCaT cell membrane after 24 h of exposure when the concentration exceeds 5 μg/mL [121]. Another study has demonstrated that CuO-NPs can penetrate the cell membrane and produce compounds that contain essential enzymes within the cells, ultimately leading to cell death [122]. Moreover, previous studies have indicated that the structure of CuO-NPs doped with various metals, including zinc, cobalt, zirconium, tungsten, and silver, enhanced the bactericidal activity against various bacteria [118,123–125]. This result can be attributed to the larger specific surface area of the metal-doped nanoparticle structure.

Some studies have demonstrated the excellent antimicrobial activity of cerium dioxide nanoparticles (CeO_2-NPs) against different strains of bacteria [126]. Gelatin polycaprolactone nanofibers containing CeO_2-NPs were developed for post-surgical topical antibacterial therapy [127]. In vitro antibacterial and cytotoxicity assays showed that the nanofibers containing 200 μg/mL of CeO_2-NPs had bactericidal activity against *P. aeruginosa* while

remaining nontoxic towards human fibroblast cells. Remarkably, the nanofiber composites observably downregulated the expression of three genes, including *shv*, *kpc*, and *imp* genes, which have been implicated in antimicrobial resistance acquisition. ROS has a critical function in disrupting the cell membrane and serves as the primary bactericidal mechanism of CeO_2-NPs [128,129]. David et al. fabricated a nanocomposite with antibacterial properties by incorporating titanium dioxide nanoparticles (TiO_2-NPs) into multi-walled carbon nanotubes [130]. The results indicate that TiO_2-NPs inhibit *S. aureus*, *E. coli*, and *C. albicans*, and remains nontoxic to human dermal fibroblasts. As a highly efficient and low-side-effect photocatalytic antibacterial agent, TiO_2 can achieve antibacterial effects through various pathways [131]. ROS produced by TiO_2 and released metal ions can induce cell membrane peroxidation and enhance its permeability, eventually leading to cell death [132–134]. Studies have shown that the bactericidal process also involves disrupting the lipid layer on the cell surface, disturbing intracellular electron transport and inactivating intracellular proteases [135,136]. The released metal ions can undergo electrostatic adsorption onto the cell membrane, damaging the cell and intracellular proteins [137]. Further research is still required to investigate the mechanism of photocatalytic antimicrobial activity. Li et al. demonstrated the excellent anti-infective activity of cobalt-NP-modified TiO_2 heterojunctions through in vitro and in vivo antibacterial experiments [138].

5. Other Inorganic Nanoparticles

Inorganic NPs are considered the next generation of new antibiotic-free antimicrobials due to their stability, easy fixation on implant surfaces, and ability to kill bacteria through multiple mechanisms [139]. In addition to metallic and metal oxide NPs, other inorganic NPs have been applied to antimicrobial coatings, such as metalloid elements, metal compounds, and hybrids. Previous studies have demonstrated that SeNPs possess anti-cancer, antioxidant, and substantial antibacterial activities against fungi and bacteria [140]. In recent years, selenium nanoparticles (SeNPs) have emerged as a promising antibacterial material in numerous studies due to their very low toxicity to mammalian cells [141–144]. As an antibacterial coating, SeNPs were deposited on titanium implants by surface-induced nucleation and showed inhibitory effects against MRSA and MRSE [145]. The NPs not only reduced the number of bacteria in the tissue surrounding the implant but also suppressed biofilm formation on the implant. Importantly, SeNPs with a zero oxidation state have been proven less toxic than other forms of Se, especially towards erythrocytes and embryonic fibroblasts [146–148]. Moreover, the SeNPs demonstrated synergistic antibacterial effects when combined with lysozyme, as high concentrations enabled effective inhibition of bacterial growth at significantly lower concentrations of SeNPs. Like most metal NPs, SeNPs induce rapid bacterial lysis by disrupting the bacterial membrane, exhibiting a similar antibacterial mechanism [149]. Furthermore, the gradual release of soluble selenium from SeNPs can effectively hinder the growth of *S. aureus* by depleting free intracellular thiols.

Guo et al. first investigated the antibacterial effects of magnesium fluoride (MgF_2) nanoparticles from the perspective of innate immunity [150]. MgF_2 nanoparticles (MgF_2-NPs) deposited on the surface of titanium implants by magnetron sputtering have been shown to possess good anti-biofilm ability in in vitro experiments, and superior anti-infection effects in vivo experiments. The study examined the co-culturing of MgF_2-NPs, bacteria, and polymorphonuclear leukocytes (PMNs), which are the primary white blood cells and vital immune cells of innate immunity. The findings demonstrated that MgF_2-NPs enhanced the antibacterial ability of PMNs by improving their phagocytic capacity and stability. The indirect immune-enhancing effect of MgF_2 can promote the host's innate immune response against bacteria. This effect was concentration-dependent. At a low concentration of 1.0–4.0 μM, fluoride significantly enhanced the ability of PMNs to phagocytose bacteria in vitro, but it inhibited the phagocytic and microbicidal abilities of PMNs at a concentration of 10–30 mM [151]. PMNs released ROS upon engulfing bacteria and formed phagosomes to eliminate bacteria [152]. Fluorine ions have been widely recognized for inhibiting bacterial metabolic activity through various mechanisms and

possessing good antibacterial properties [153]. It has been observed that the excellent anti-biofilm activity of Mg fluoride nanofilms may be due to the fluorine ions released from the nanofilms. Nevertheless, the specific molecular mechanism requires further investigation. Moreover, the fluorine ions released from MgF_2-NPs did not hinder the proliferation of fibroblasts while exerting antibacterial effects [154], and even promoted osseointegration in vivo and osteogenesis in vitro [155,156]. However, additional studies have indicated that free MgF_2-NPs, rather than the released fluorine ions, have antibacterial functions against *S. aureus* and *E. coli* [157]. MgF_2-NPs can inhibit the activity of *E. coli* F_1-ATPase by forming MgADP-MgFx complexes [158]. A thin film of MgF_2-NPs can prevent bacterial adhesion, and the released NPs prevent bacterial biofilm formation through contact inhibition [159].

Stubborn bacterial biofilms and pervasive antibiotic resistance pose significant global threats to human health. Therefore, there is an urgent need for an implant nanomaterial with multiple antimicrobial modalities, thereby combining the ability of biofilm destruction and the low risk of bacterial resistance. MXene materials are a type of metal carbide and metal nitride material with two-dimensional (2D) layered structures and have many superior properties, including the tunability of elemental composition and structure, metallic properties, carrier migration anisotropy, and good optical and mechanical properties [160]. These materials have gained global attention across various fields (such as energy storage, biomedicine, catalysis, etc.) [161,162]. Furthermore, they also exhibit excellent antibacterial properties influenced by ultrathinness and atomic structures, according to some studies [163]. A 2D niobium carbide (Nb_2C) MXene titanium plate (Nb_2C@TP)-based medical implant with bacterial clearance and tissue regeneration capacities was developed for multimodal infection control (Figure 3) [164]. The results indicate that Nb_2C MXene nanosheets (NSs) as an antibiofilm implant surface modification can effectively inhibit bacterial biofilm formation and induce bacterial apoptosis. Multiple antimicrobial mechanisms, including biofilm inhibition, intrinsic bactericidal features, and photothermal bacteria ablation, are involved in the antibacterial activity of Nb_2C@TP. These were summarized as follows: (1) Down-regulating the bacterial energy metabolism pathways leads to the destruction of biofilms and elimination of bacteria. Nb_2C@TP promotes biofilm separation by activating the accessory gene regulator (Agr), which is critical for bacterial–biofilm interaction [165,166]. It can also significantly suppress the expression of genes related to bacterial energy metabolism, which are essential for bacterial growth and proliferation. These findings suggested that Nb_2C@TP had a significant effect on bacterial metabolism. (2) Nb_2C@TP directly leads to bacterial death through down-regulation of the tricarboxylic acid cycle and phosphotransferase system pathway. Direct physical interaction between the sharp edges of NSs and the bacterial membrane surface can disrupt the bacterial cell membrane, ultimately resulting in its death [167]. (3) Due to the excellent photothermal conversion efficiency and the sensitization ability toward bacteria of Nb2C@TP, a physical thermal shock was employed to eliminate planktonic bacteria by denaturing DNA and proteins, disrupting the bacterial motor system, and inducing efflux of cytoplasm from the bacterial membrane. Shedding of cilia and flagella from the bacterial membrane can be observed under a transmission electron microscope, suggesting that physical thermal shock can destroy bacterial structures, prevent bacteria spread, and prevent biofilm formation, ultimately leading to bacteria death. Because of the heightened heat sensitivity of bacteria, the current study employed reduced heat levels to minimize the potential side effects of hyperthermia.

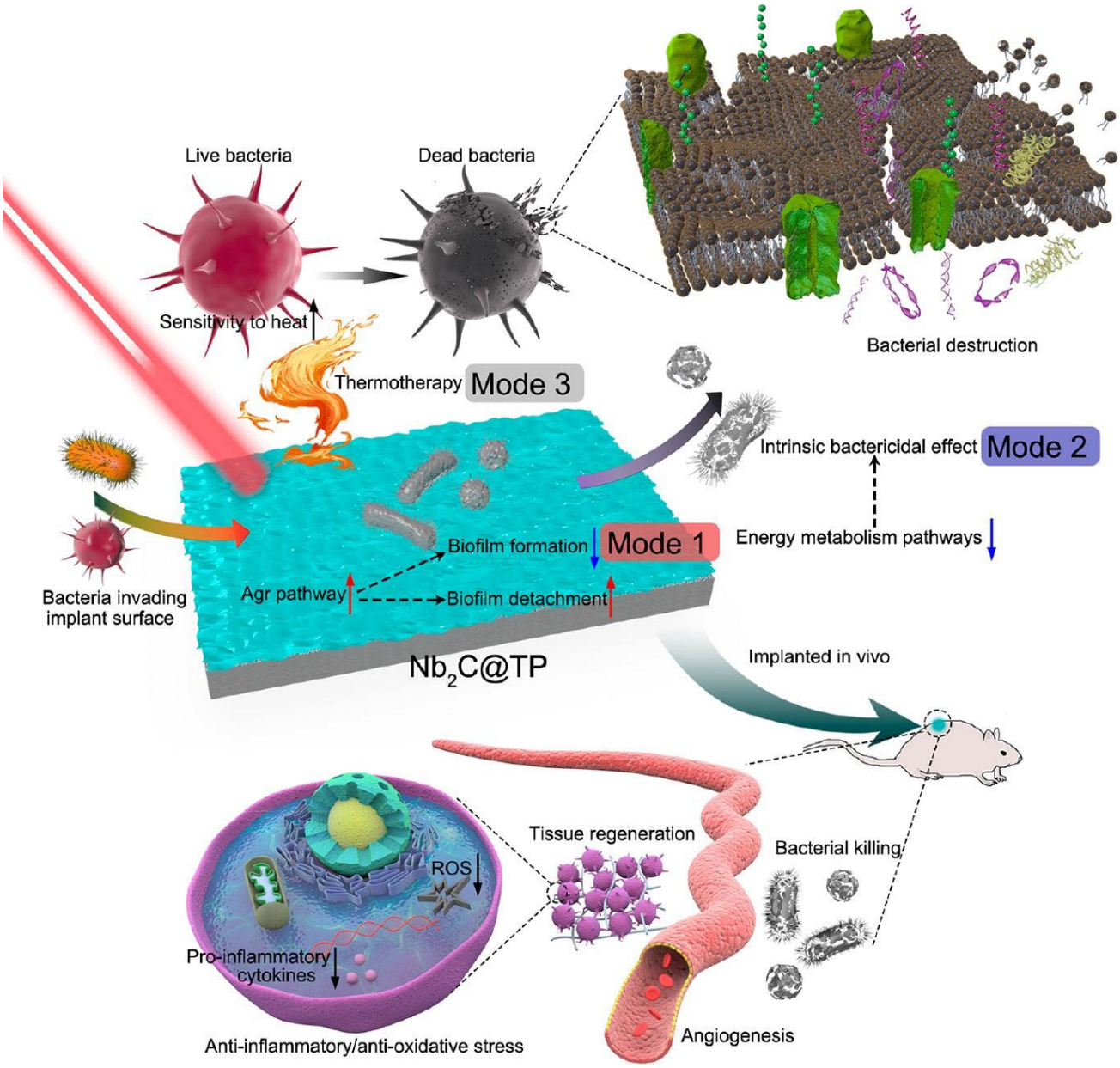

Figure 3. Nb2C@TP with three bacterial clearance strategies and tissue regeneration capabilities. The upward solid arrows in the figure represent up-regulation and the downward solid arrows represent down-regulation. Reprinted with permission from Ref. [164]. Copyright 2021 American Chemical Society.

6. Organic Nanoparticles

Polyetheretherketone (PK) is widely used in orthopedic surgery due to its good biological and physical properties [168]. PK as a bioinert material leads to low cell adhesion and growth, as well as the loss of bone bonding after implantation. In recent years, many PK-based nanocomposites have been endowed with biological activity and antibacterial properties [156]. Tang et al. [169] prepared a nano zinc-magnesium silicate (nZMS)/PK bioactive composite (nZPC) to improve the bioactivity and antibacterial properties of PK as a bone implant. With increased nZMS content, nZPC significantly enhanced cell attachment, proliferation, and osteogenic differentiation. Zinc ions released by nZMS show antimicrobial properties through their synergistic effects on bacterial membranes and membrane proteins, as well as intracellular enzymes [170]. Moreover, zinc ions exert antimicrobial activity by disrupting the enzymes responsible for electron transfer and

inhibiting bacterial DNA replication [171,172]. The study suggested that nZPC containing 50 w% of nZMS (50nZPC) exhibits good bioactivity and antibacterial activity, indicating its potential as a promising antibacterial material for orthopedic implants.

Compared with antibiotics and metal NPs, natural antimicrobial peptides (AMP) exhibit excellent antibacterial activity while avoiding drug resistance. AMPs can eliminate bacteria by interacting electrostatically with the anionic cell membranes of bacteria through their cationic groups, as well as by disrupting nonpolar bacterial membranes using hydrophobic residues [173]. The hydrophobic-modified antimicrobial peptides have many advantages, including multi-biological functions, broad-spectrum antibacterial ability, and low production cost. Research shows that quaternized polycarbonates not only have good biocompatibility and biodegradability, but can inhibit bacterial growth by interacting with bacterial membranes [174,175]. A previous study indicated that PEGylated polycaprolactone with cationic arms provided more surface-positive charges on the NPs, which was essential for improving antimicrobial activity [176–178]. A new type of comb-like amphiphilic cationic polycarbonate was prepared and blocked onto the polyethylene glycol (PEG) by side chain atom transfer radical polymerization (ATRP) to exert antimicrobial efficacy against Gram-negative and Gram-positive bacteria [179]. Moreover, the efficacy of comb-like cationic polycarbonates with hydrophobically modified polyquaternium side chains (G-CgQAs) in fighting vancomycin-resistant bacteria in mice has been demonstrated. The antimicrobial activity of G-CgQAs results from strong hydrophobic and electrostatic interactions, which can be mediated by the added hydrophobic poly(n-BMA)-segments with a lipopolysaccharide (LPS) layer on the surface of bacteria [180,181]. The results demonstrated that the interactions of G-CgQAs NPs with bacteria disrupt the membrane structure, further leading to bacterial death. Nevertheless, it is vital to assess the biocompatibility and biodegradability of these antibacterial polymers in their clinical application, which was not addressed in this study.

It is worth mentioning that integrating the functional components of multifunctional organic nanocoatings into one layer can result in reduced surface properties, increased production costs, and increased burden for material property control because of the decrease in surface-grafting density for each component [182,183]. Therefore, organic biological coatings with simple molecular structures and high surface-grafting density represent future implant material coatings development trends. One study reported that a sulfonate-based anionic polypeptide (PLC-SO_3X, X=Na, H) coating with biocompatibility, antibacterial, and antifouling properties was fabricated through ring-opening polymerization of L-cysteine-based N-carboxyanhydride (NCA) with allyl groups and the thiol–ene reaction [184]. The antibacterial mechanism of PLC-SO_3X depends on the formation of a local acidic environment for the sulfonic acid side chain [185,186]. Furthermore, higher surface density of the sulfonic acid group results in a more substantial bactericidal effect. PLC-SO_3X can self-assemble into spherical NPs through intermolecular H-bonding interactions from the β-sheet conformation, which can improve the local functional group density and enhance the antibacterial activity [187]. Furthermore, the sulfonic acid group on the surface of the NPs can inhibit bacterial adhesion [188]. The polypeptide coating used as an anti-infective coating on implant materials exhibits good antibacterial properties, biocompatibility, and antifouling ability. However, polymers containing sulfonic acid groups are highly cytotoxic to mammalian cells [189]. The present study has demonstrated that PLC-SO_3Na has negligible cytotoxicity on erythrocytes but slight cytotoxicity on HEK 293T cells, possibly due to the anionic peptides inducing cell membrane disorder and cell death. Thus, further studies are needed to determine its cytotoxicity.

7. Nanoscale Surface with Special Morphology

Nanoparticles have been extensively investigated as antibacterial materials for orthopedic implants. More and more researchers are concerned that the surface topography of implants can also inhibit the adhesion of microorganisms, or even kill them. The development of antimicrobial nanosurfaces shows promising applications in orthopedic implants.

The physico–biochemical interactions between these nanomorphologies and the microorganisms inhibit microbial adhesion and biofilm formation, thus enhancing the antibacterial effect of the implant material itself. In research aiming to exert an antibacterial effect by inhibiting bacterial adhesion at the very beginning, the construction of nanomorphology characteristics has gradually become a new direction for implants.

7.1. Nanopillars

In orthopedic implant infection prevention, an increasing number of investigators have focused on preventing the initial attachment of bacteria to the implant surface. Recently, researchers have been exploring the modification of material surfaces to confer antifouling or bactericidal capabilities, thereby preventing bacterial cell attachment and enabling the substratum to kill bacteria mechanically. The nanopillars on the substrate surface can provide unfavorable attachment points to prevent microbial colonization and mechanically dissolve any bacterial cells that encounter the surface [190]. The bactericidal properties of the nanopillars result from mechanical disruption of the bacterial cell membrane. Nanopillars can induce the stretching and rupture of the bacterial membrane while cleaving it with their sharp edges [27]. However, the specific bactericidal mechanism varies depending on the geometry of the different nanopillars. Researchers discovered that the adhesion forces generated by the nanopillar arrays on an insect's wing surface could deform the attached bacteria, causing the rupture of their cell membranes and subsequent bacterial cell death [191,192]. This discovery has stimulated research on synthesizing biomimetic nanomaterials that have emerged as a promising technology for the surface sterilization of implants. It was found that the bactericidal effect of highly ordered nanopillar arrays with a high aspect ratio is determined by the relative flexibility of individual nanopillars and the mechanical energy stored within them [193]. When bacteria adhere to the substrate surface, the resulting elastic pillar deformations lead to lateral stretching of the cell membrane and interactions at the cell edge. At a height of 360 nm, relative to 220 and 420 nm, the pillars are elastic enough to bend in response to bacterial membrane adsorption, thus exhibiting the highest degree of antimicrobial activity. The stress-induced deflection of the nanopillars upon bacterial membrane adsorption resulted in an enhanced bactericidal effect against both Gram-negative and Gram-positive bacteria. The nanostructured surfaces of these insect-wing-like structures induce the stretching and rupture of the bacterial cell wall through the interplay of intrinsic adhesion to the cell wall and its elastic deformation. Moreover, the cell wall that is adsorbed onto the nanopillar of the matrix experiences mechanical stress, resulting in an elevation of internal turgor pressure, thereby causing the cell wall to become hardened. The sensitivity of bacteria to nanopillar-surface physical-mechanical sterilization is mainly affected by cell wall hardness and other cell mechanical properties [194]. It facilitates the comprehension of the notable variations in bactericidal effects among different bacteria when interacting with the same substrate. In addition, the fundamental parameters affecting the bactericidal effect of the substrate surface included the spacing, height, tip diameter, and base diameter of the nanopillars. The bactericidal activity of nanopillars was enhanced with the increase in their height and sharpness [195]. Increasing the density of the nanopillar resulted in an increase in the total area of the bacterial membrane adsorbed on it, leading to a better stretch of the cell membrane [196].

It was found that the elastic energy stored in the flexible nanopillars could be released upon their deflection and contraction, enhancing their ability to stretch the bacterial cell membrane. The mechano-bactericidal effect of multi-walled carbon nanotubes (CNTs) is derived from the stored elastic energy due to deflection and contraction of the nanopillar tip upon bacterial adsorption [197].

The sharp edges of the nanopillars can also exhibit high bactericidal activity [198]. Graphene nanosheets were observed to induce local disruption of the bacterial cell membrane, loss of membrane potential, alterations in osmotic pressure, and leakage of cytoplasm [199]. Likewise, sharp nanoneedles on mechano-bactericidal silicon surfaces not only

possess bactericidal properties, but also contribute to reducing inflammatory responses in mice [200].

7.2. Nanohole

The application of antibacterial nanomaterials in bone infection has become a rapidly growing field. The generation of ROS and disruption of bacterial cell membranes are commonly considered classic antibacterial mechanisms. [201]. In contrast to the currently understood primary antibacterial mechanism, a novel concept regarding the antimicrobial mechanism of nanohole-boosted electron transport (NBET) has been recently proposed [202]. Nanoholes with atomic vacancies and biofilms act as electron donors and receptors, enhancing the high electron transfer capacity between nanomaterials and biofilms. Electron transport disrupts the bacterial biofilm by damaging the key components, such as proteins, polysaccharides, and extracellular DNA, on its surface. The nanoholes have been shown to effectively decrease the expression of genes associated with biofilm formation, leading to increased cell permeability and inhibition of biofilm synthesis. The nanohole-enriched MoS_2 (NR-MoS_2) exhibited excellent in vitro and in vivo anti-infection efficacy, surpassing both traditional antibiotics and other antibacterial nanomaterials in terms of biocompatibility (Figure 4). After 10 consecutive generations, *S. aureus* exhibited rapid development of resistance to common antibiotics, up to 125–268-fold. However, resistance to NR-MoS2 did not emerge, even after 20 consecutive generations.

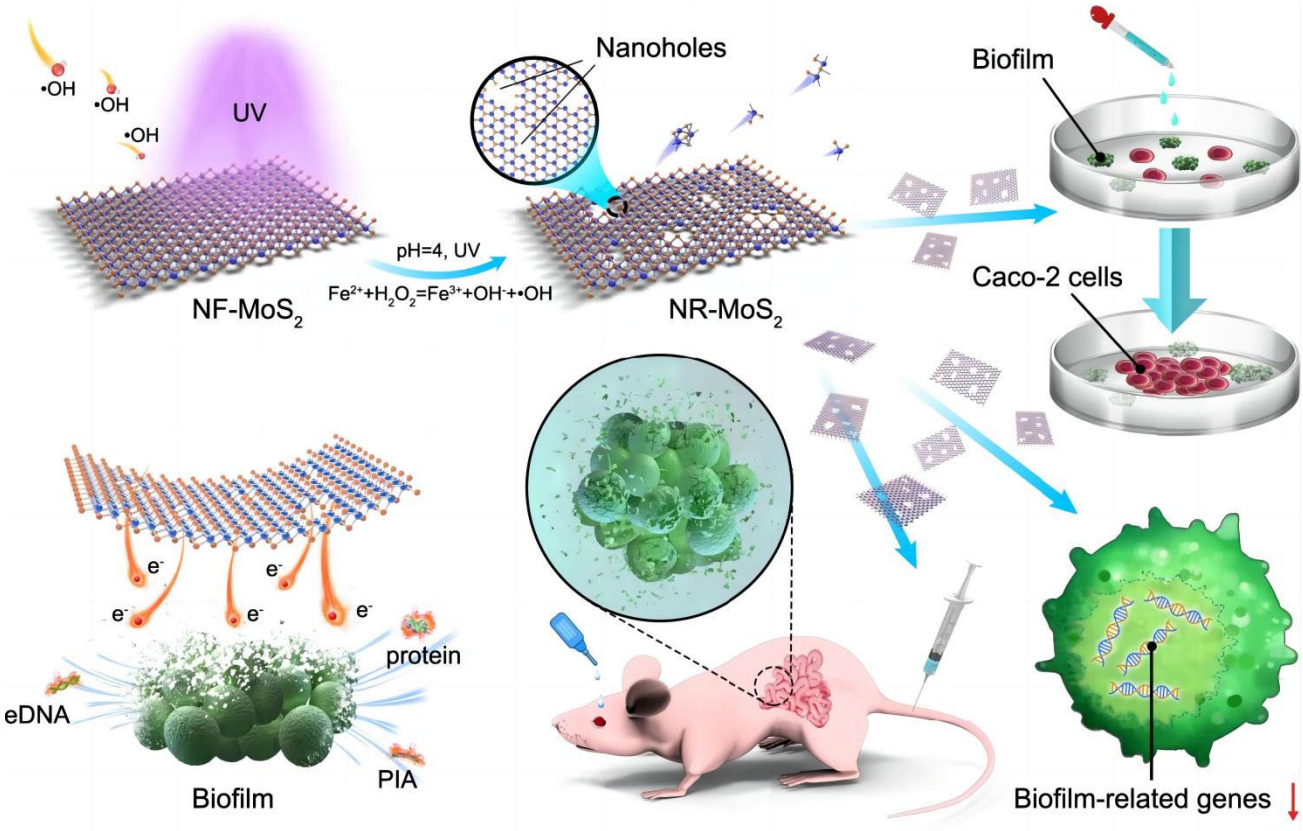

Figure 4. Schematic diagram of the nanohole-boosted electron transport (NBET) and the anti−infective mechanisms in vitro and in vivo. Reprinted with permission from Springer Nature. This is an open access article.

7.3. Nanomaterials of Other Shapes

Bacterial biofilms are well known for their ability to create physical barriers and immunosuppressive microenvironments, protecting bacteria from antimicrobial agents and hindering the host immune response [5,203]. Biofilm formation can transform macrophages into an anti-inflammatory phenotype, reducing their bactericidal activity and impeding

biofilm clearance [204,205]. Overcoming these barriers is crucial for effective sterilization. A new approach called space-selective chemodynamic therapy has been proposed, using $CuFe_5O_8$ nanocubes (NCs) as catalysts for pH- and H_2O_2 concentration-dependent Fenton-like reactions to continuously eliminate biofilm fragments and exposed bacteria [206]. It is exciting to discover that this nanomaterial, based on dual transition metals (Fe and Cu), can overcome the physical and chemical barriers that induce the immunosuppressive microenvironment. This study has demonstrated that the Fenton-like reactions catalyzed by $CuFe_5O_8$ NCs generate significantly higher levels of ROS within the biofilm, compared to lower levels of ROS outside the biofilm. The high levels of hydroxyl radicals catalyzed by $CuFe_5O_8$ NCs can cleave extracellular DNA (eDNA) and disrupt the bacterial biofilm. However, the low levels of hydroxyl radicals can stimulate the production of diverse pro-inflammatory cytokines, consequently bolstering the inflammatory response against infection and facilitating pathogen elimination [207,208]. Outside the biofilm, the immunosuppressive microenvironment is effectively reversed, since low levels of ROS can activate pro-inflammatory immunity and produce low levels of hydroxyl radicals with relatively high pH and low H_2O_2. Therefore, $CuFe_5O_8$ NCs not only disrupt the biofilm to kill bacteria but also exhibit an immunity-remodeling effect by activating local macrophage-associated immunity. Thus, they are considered a practical approach to combatting biofilm infections related to implants. Guo et al. suggested that the antibacterial activity of $CuFe_5O_8$ NCs may have originated from eDNA cleavage induced by the generation of hydroxyl radicals, effectively disrupting the bacterial biofilm. In addition to direct bactericidal effects, they inhibit bacterial adhesion and split biofilms, contributing to their anti-biofilm activity. The role of immune regulation in biofilm-associated infections has often been overlooked in previous studies. Following the disruption of the biofilm structure, $CuFe_5O_8$ NCs induced the differentiation of macrophages into M1 macrophages and promoted the release of pro-inflammatory cytokines to eliminate the biofilm. Additionally, $CuFe_5O_8$ NCs reversed the polarization of M2 macrophages, which is typically induced by the biofilm, and created a new pro-inflammatory microenvironment around the prosthetic area. Similarly, palladium (Pd) nanocrystals have demonstrated excellent antibacterial properties by generating reactive oxygen species through their oxidase- and peroxidase-like activities [56].

Multi-walled carbon nanotubes (MWCNTs) have been employed in antimicrobial and drug delivery applications [209,210]. Surface modification of MWCNTs endows these materials with new properties. For example, the presence of NPs on their surface can significantly enhance the antimicrobial activity of MWCNTs [211]. Recent research also showed that different types of NP-modified MWCNTs exhibit higher antimicrobial activity [212]. Through their synergistic effect, MWCNTs decorated with AgNPs and ZnO NPs showed more potent antibacterial activity against *E. coli*, *S. aureus*, *B. subtilis*, and *P. aeruginosa*. Similarly, combining ZnO NPs with MWCNTs improved the antibacterial properties of the nanocomposites against *E. coli*. In in vitro antibacterial experiments, MWCNTs_ZnO and MWCNTs_Ag demonstrated significant antibacterial activity, even at lower concentrations of 0.015% and 0.007%, respectively, resulting in observable inhibition.

Table 1. Bactericidal activity of nanostructured surfaces.

Material	Morphology	Bactericidal Mechanisms	Dimensions	Tested Organism	Biological Activity/Effect/Outcome	Refs.
PDA	Nanoparticles	Release of NOR and CEP	NA	*S. aureus* and *P. aeruginosa*	Antibiotic-embedded superhydrophilic coating (PDA/NOR and PDA/CEP) possessed the reinforced antibacterial ability.	[34]

Table 1. *Cont.*

Material	Morphology	Bactericidal Mechanisms	Dimensions	Tested Organism	Biological Activity/Effect/Outcome	Refs.
Chitosan	Nanopores	Release of Bbr	Less than 1 μm	*S. aureus*	The inhibition area in the Bbr/CMCSM group suggested a significant antimicrobial activity.	[35]
LbL films composed of CBSA NPs and OSA	Nanoporous	Release of VAN	Nanoporous structures	*S. epidermidis*	VAN-loaded LbL films showed excellent antibacterial activity.	[36]
Ti-NT	Nanotube	Release of VAN	100 nm in diameter	*S. aureus*	The Ti-NT-VAN/pDA/Hya exhibited better antibacterial activity.	[38]
Halloysite clay nanotubes	Nanotube	Release of MNA	A diameter of 50 nm and a length of 600 nm	*Fn*	The nanotube composite inhibits bacterial growth in an area larger than the membrane size and keeps the inhibition zone long.	[41]
MSNs	Nanoparticles	Release of VAN	100 nm in diameter	*MRSA*	The PEG-D6- and PEG-UBI29-41-modified MSN nanocomposites possessed excellent antibacterial activity.	[48]
MSNs	Nanoparticles	Release of Lev	NA	*E. coli* and *S. aureus*	The composite scaffold significantly inhibited the growth of both *E. coli* and *S. aureus*.	[49]
PCL/gelatin	Nanofibers	Release of MNA	560 nm in average diameter	*Fn* and *Pg*	The bacterial inhibition zones are observed around the membrane for the bacterial nanofibers with core-shell structure.	[51]
Silver	Nanoparticles	Ionic silver and reactive oxygen species (ROS)	40–80 nm	*E. coli* and *S. epidermidis*	The antibacterial rates for adhered bacteria were maintained at 89.9% and 93.5%, respectively, for *S. aureus* and *E. coli* within 12 weeks.	[71]
Cu/Ag-PDA-NPs	Nanoparticles	Ionic copper and silver and reactive oxygen species (ROS)	270 ± 28 nm	*S. mutans*, *P. aeruginosa*, *E. coli*, and *S. aureus*	The marked antimicrobial activities against *S. mutans*, *P. aeruginosa*, *E. coli*, and *S. aureus*.	[84]
BGz	Nanospheres	Attachment to the cell membrane, accumulation in the cytoplasm, and the production of ROS	282.8 ± 2.1 nm	*P. gingivalis*	*P. gingivalis* was significantly reduced in the BGz group.	[88]

Table 1. *Cont.*

Material	Morphology	Bactericidal Mechanisms	Dimensions	Tested Organism	Biological Activity/Effect/Outcome	Refs.
Gold	Nanoparticles	Gold ions penetrate the membrane and cell wall, resulting in bacterial death	33 nm in average diameter	*S. epidermidis* and *Klebsiella* spp.	Over 99.99% of the colonies and the colony forming units, including *Klebsiella* spp. and *S. epidermidis*, were eliminated at 0.64 wt% of AuNPs.	[96]
ZnO	Nanoparticles	Nanoparticle internalization, membranolysis, and ROS generation	18 ± 5 nm	*S. aureus* and *E. coli*	The viability of *S. aureus* and *E. coli* bacterial cells was reduced by 65% and 10%, respectively.	[70]
CuO	Nanoparticles	Generation of ROS	NA	*S. aureus*, *P. aeruginosa*, and *E. coli*	The bactericidal activity was observed for both Gram-positive and Gram-negative bacteria.	[117]
CeO_2	Nanoparticles	Cell membrane damage caused by ROS	≤20 nm	*P. aeruginosa*	CNPs in a solution at a concentration of 200 µg/mL had bactericidal activity against *P. aeruginosa*.	[127]
TiO_2	Nanoparticles	NA	15 nm in diameter	*S. aureus*, *E. coli*, and *C. albicans*	It inhibited the growth of *S. aureus* and *E. coli*, as well as *C. albicans*.	[130]
Se	Nanoparticles	Destruction of bacterial membranes to induce rapid cell lysis	30–70 nm	*MRSA* and *MRSE*	The decrease in bacterial cell viability of MRSA and MRSE can be attributed to a decrease in the number of bacterial cells.	[145]
MgF_2	Nanoparticles	Direct antimicrobial effects of MgF2-NPs enhancing the phagocytosis of PMNs	NA	*MRSA*, *S. epidermidis*, and *S. aureus*	MgF_2 nanoparticle films significantly restricted the biofilm formation in a dose-dependent manner.	[150]
Nb_2C	Nanosheets	Biofilm inhibition, intrinsic bactericidal and photothermal bacteria ablation	Average size of ~150 nm	*MRSA* and *E. coli*	Nb_2C@TP can effectively eradicate planktonic bacteria and inhibit biofilm formation.	[164]
G-CgQAs	Nanoparticles	Positive charge and suitable hydrophobic–hydrophilic balance	60 nm	*S. aureus*, *MRSA*, and *E. coli*	It not only has a broad spectrum and high antimicrobial activity against Gram-negative, Gram-positive, and antibiotic-resistant bacteria, but also shows strong anti-infective effects against vancomycin-resistant bacteria.	[179]

Table 1. *Cont.*

Material	Morphology	Bactericidal Mechanisms	Dimensions	Tested Organism	Biological Activity/Effect/Outcome	Refs.
PLC-SO_3X	Nanoparticles	The low local pH from sulfonic acid side chains	50 nm	*S. aureus* and *E. coli*	The sterilization rate of the PLC-SO_3H coating against *S. aureus* and *E. coli* were 99.1% and >99.9%, respectively.	[184]
nZMS	Nanoparticles	Release of zinc ions	100 nm	*E. coli*	The nZPC revealed good antibacterial activity against *E. coli*, in which 50nZPC had the strongest antibacterial activity.	[169]
Silicon	Nanopillars	Stress-induced deflection of the nanopillars	360 nm	*P. aeruginosa* and *S. aureus*	The 360 nm nanopillar array exhibited the highest antimicrobial activity, resulting in 95 ± 5% and 83 ± 12% cell death of *P. aeruginosa* and *S. aureus*, respectively.	[193]
NR-MoS_2	Nanohole	Facilitation of electron transport	40 nm	*S. aureus*	The anti-infection capacity of the NR-MoS2 was found to be excellent, both in vitro and in vivo.	[202]
$CuFe_5O_8$	Nanocubes	Generation of ROS; remodeling of the immune microenvironment	A mean side length of about 15 nm	*S. aureus* and *E. coli*	$CuFe_5O_8$ NCs effectively ruin the bacterial cell wall or membranes of *S. aureus* and *E. coli* planktonic bacteria.	[206]
MWCNTs	Nanotubes	The physical interaction of the nanomaterials with cell membranes, disruption of cell membranes and DNA structures.	7–33 nm	*E. coli*, *S. aureus*, *B. subtilis*, *C. albicans*, and *P. aeruginosa*	The nanocomposites show obvious antibacterial activity and reduce biofilm formation in multiple associated microbial strains.	[212]

S. aureus, *Staphylococcus aureus*; *S. epidermidis*, *Staphylococcus epidermidis*; *Fn*, *Fusobacterium nucleatum*; *MRSA*, *Methicillin-resistant Staphylococcus aureus*; PCL, polycaprolactone; *Pg*, *Porphyromonas gingivalis*; *E. coli*, *Escherichia coli*; *S. mutans*, *Streptococcus mutans*; *P. aeruginosa*, *Pseudomonas aeruginosa*; BGz, Bioactive glass; *P. gingivalis*, *Porphyromonas gingivalis*; CuO, cupric oxide; CNPs, cerium oxide nanoparticles; *MRSE*, *Methicillin-resistant Staphylococcus epidermidis*; *C. albicans*, *Candida albicans*.

8. Summary

With advancements in nanotechnology, antibacterial orthopedic implants have made significant progress. Nanomaterials have demonstrated significant advantages over antibiotics regarding biocompatibility and reduction of antibiotic resistance. This study overviews recent research on antimicrobial nanomaterials in orthopedic implants. Nanotechnology offers various therapeutic approaches for preventing and treating infections in orthopedic surgery. Continuous innovation and improvement of nanomaterials are necessary to address severe postoperative infections. Moreover, nanomaterials can enhance biocompatibility and exhibit different biological functions through loading with proteins and drugs. Despite the great potential of nanomaterials in antibacterial therapy for ortho-

pedic implants, there is currently a lack of commercially available products that are easily transformed and cost-effective.

Author Contributions: J.S., Conceptualization, investigation, methodology, writing—original draft preparation, writing—review, and editing; Y.H., conceptualization, investigation, writing—original draft preparation, writing—review, and editing; M.C., conceptualization, investigation, methodology, writing—original draft preparation; Z.Z., investigation, data curation; X.M., investigation, data curation; L.L., investigation, data curation; S.H., conceptualization, methodology, supervision; S.L., conceptualization, methodology, supervision; H.Z., conceptualization, methodology, supervision. All authors have read and agreed to the published version of the manuscript.

Funding: This research was supported by the Shanghai Science and Technology Innovation Action Plan [Grant No. 22S31900400].

Institutional Review Board Statement: The study did not require ethical approval.

Informed Consent Statement: All images are approved for publication.

Data Availability Statement: All data that support the findings of this study are included within the article.

Conflicts of Interest: The authors declare that they have no conflicts of interest.

References

1. McCloskey, A.P.; Gilmore, B.F.; Laverty, G. Evolution of antimicrobial peptides to self-assembled peptides for biomaterial applications. *Pathogens* **2014**, *3*, 791–821. [CrossRef] [PubMed]
2. Tan, L.; Li, J.; Liu, X.; Cui, Z.; Yang, X.; Zhu, S.; Li, Z.; Yuan, X.; Zheng, Y.; Yeung, K.W.K.; et al. Rapid Biofilm Eradication on Bone Implants Using Red Phosphorus and Near-Infrared Light. *Adv. Mater.* **2018**, *30*, e1801808. [CrossRef] [PubMed]
3. Costerton, J.W.; Stewart, P.S.; Greenberg, E.P. Bacterial biofilms: A common cause of persistent infections. *Science* **1999**, *284*, 1318–1322. [CrossRef] [PubMed]
4. Zimmerli, W.; Trampuz, A.; Ochsner, P.E. Prosthetic-joint infections. *N. Engl. J. Med.* **2004**, *351*, 1645–1654. [CrossRef] [PubMed]
5. Arciola, C.R.; Campoccia, D.; Montanaro, L. Implant infections: Adhesion, biofilm formation and immune evasion. *Nat. Rev. Microbiol.* **2018**, *16*, 397–409. [CrossRef] [PubMed]
6. Azeredo, J.; Azevedo, N.F.; Briandet, R.; Cerca, N.; Coenye, T.; Costa, A.R.; Desvaux, M.; Di Bonaventura, G.; Hébraud, M.; Jaglic, Z.; et al. Critical review on biofilm methods. *Crit. Rev. Microbiol.* **2017**, *43*, 313–351. [CrossRef]
7. Higgins, C.F. Multiple molecular mechanisms for multidrug resistance transporters. *Nature* **2007**, *446*, 749–757. [CrossRef]
8. Holmes, A.H.; Moore, L.S.P.; Sundsfjord, A.; Steinbakk, M.; Regmi, S.; Karkey, A.; Guerin, P.J.; Piddock, L.J.V. Understanding the mechanisms and drivers of antimicrobial resistance. *Lancet* **2016**, *387*, 176–187. [CrossRef]
9. Ikuta, K.S.; Swetschinski, L.R.; Aguilar, G.R.; Sharara, F.; Mestrovic, T.; Gray, A.P.; Weaver, N.D.; Wool, E.E.; Han, C.; Hayoon, A.G.; et al. Global mortality associated with 33 bacterial pathogens in 2019: A systematic analysis for the Global Burden of Disease Study 2019. *Lancet* **2022**, *400*, 2221–2248. [CrossRef]
10. Fang, G.; Li, W.; Shen, X.; Perez-Aguilar, J.M.; Chong, Y.; Gao, X.; Chai, Z.; Chen, C.; Ge, C.; Zhou, R. Differential Pd-nanocrystal facets demonstrate distinct antibacterial activity against Gram-positive and Gram-negative bacteria. *Nat. Commun.* **2018**, *9*, 129. [CrossRef]
11. Zou, W.; Zhou, Q.; Zhang, X.; Hu, X. Environmental Transformations and Algal Toxicity of Single-Layer Molybdenum Disulfide Regulated by Humic Acid. *Environ. Sci. Technol.* **2018**, *52*, 2638–2648. [CrossRef] [PubMed]
12. Li, B.; Webster, T.J. Bacteria antibiotic resistance: New challenges and opportunities for implant-associated orthopedic infections. *J. Orthop. Res.* **2018**, *36*, 22–32. [CrossRef]
13. Blair, J.M.A.; Webber, M.A.; Baylay, A.J.; Ogbolu, D.O.; Piddock, L.J.V. Molecular mechanisms of antibiotic resistance. *Nat. Rev. Microbiol.* **2015**, *13*, 42–51. [CrossRef]
14. Feng, G.; Cheng, Y.; Wang, S.-Y.; Borca-Tasciuc, D.A.; Worobo, R.W.; Moraru, C.I. Bacterial attachment and biofilm formation on surfaces are reduced by small-diameter nanoscale pores: How small is small enough? *NPJ Biofilms Microbiomes* **2015**, *1*, 15022. [CrossRef]
15. Wu, S.; Zuber, F.; Brugger, J.; Maniura-Weber, K.; Ren, Q. Antibacterial Au nanostructured surfaces. *Nanoscale* **2016**, *8*, 2620–2625. [CrossRef] [PubMed]
16. Jahed, Z.; Lin, P.; Seo, B.B.; Verma, M.S.; Gu, F.X.; Tsui, T.Y.; Mofrad, M.R.K. Responses of *Staphylococcus aureus* bacterial cells to nanocrystalline nickel nanostructures. *Biomaterials* **2014**, *35*, 4249–4254. [CrossRef] [PubMed]
17. Liu, L.; Ercan, B.; Sun, L.; Ziemer, K.S.; Webster, T.J. Understanding the Role of Polymer Surface Nanoscale Topography on Inhibiting Bacteria Adhesion and Growth. *ACS Biomater. Sci. Eng.* **2016**, *2*, 122–130. [CrossRef]
18. Kim, S.; Jung, U.T.; Kim, S.-K.; Lee, J.-H.; Choi, H.S.; Kim, C.-S.; Jeong, M.Y. Nanostructured multifunctional surface with antireflective and antimicrobial characteristics. *ACS Appl. Mater. Interfaces* **2015**, *7*, 326–331. [CrossRef]

19. Ma, Z.; Ren, L.; Liu, R.; Yang, K.; Zhang, Y.; Liao, Z.; Liu, W.; Qi, M.; Misra, R. Effect of Heat Treatment on Cu Distribution, Antibacterial Performance and Cytotoxicity of Ti–6Al–4V–5Cu Alloy. *J. Mater. Sci. Technol.* **2015**, *31*, 723–732. [CrossRef]
20. Luo, F.; Tang, Z.; Xiao, S.; Xiang, Y. Study on properties of copper-containing austenitic antibacterial stainless steel. *Mater. Technol.* **2019**, *34*, 525–533. [CrossRef]
21. Nune, K.C.; Somani, M.C.; Spencer, C.T.; Misra, R. Cellular response of *Staphylococcus aureus* to nanostructured metallic biomedical devices: Surface binding and mechanism of disruption of colonization. *Mater. Technol.* **2017**, *32*, 22–31. [CrossRef]
22. Wang, L.; Chen, Y.P.; Miller, K.P.; Cash, B.M.; Jones, S.; Glenn, S.; Benicewicz, B.C.; Decho, A.W. Functionalised nanoparticles complexed with antibiotic efficiently kill MRSA and other bacteria. *Chem. Commun.* **2014**, *50*, 12030–12033. [CrossRef]
23. Gao, W.; Chen, Y.; Zhang, Y.; Zhang, Q.; Zhang, L. Nanoparticle-based local antimicrobial drug delivery. *Adv. Drug Deliv. Rev.* **2018**, *127*, 46–57. [CrossRef]
24. Blanchemain, N.; Laurent, T.; Chai, F.; Neut, C.; Haulon, S.; Krump-konvalinkova, V.; Morcellet, M.; Martel, B.; Kirkpatrick, C.J.; Hildebrand, H.F. Polyester vascular prostheses coated with a cyclodextrin polymer and activated with antibiotics: Cytotoxicity and microbiological evaluation. *Acta Biomater.* **2008**, *4*, 1725–1733. [CrossRef] [PubMed]
25. Zelken, J.; Wanich, T.; Gardner, M.; Griffith, M.; Bostrom, M. PMMA is superior to hydroxyapatite for colony reduction in induced osteomyelitis. *Clin. Orthop. Relat. Res.* **2007**, *462*, 190–194. [CrossRef]
26. Alvarez, M.M.; Aizenberg, J.; Analoui, M.; Andrews, A.M.; Bisker, G.; Boyden, E.S.; Kamm, R.D.; Karp, J.M.; Mooney, D.J.; Oklu, R.; et al. Emerging Trends in Micro- and Nanoscale Technologies in Medicine: From Basic Discoveries to Translation. *ACS Nano* **2017**, *11*, 5195–5214. [CrossRef]
27. Linklater, D.P.; Baulin, V.A.; Juodkazis, S.; Crawford, R.J.; Stoodley, P.; Ivanova, E.P. Mechano-bactericidal actions of nanostructured surfaces. *Nat. Rev. Microbiol.* **2021**, *19*, 8–22. [CrossRef]
28. Wei, T.; Yu, Q.; Zhan, W.; Chen, H. A Smart Antibacterial Surface for the On-Demand Killing and Releasing of Bacteria. *Adv. Healthc. Mater.* **2016**, *5*, 449–456. [CrossRef] [PubMed]
29. Huang, L.; Zhang, L.; Xiao, S.; Yang, Y.; Chen, F.; Fan, P.; Zhao, Z.; Zhong, M.; Yang, J. Bacteria killing and release of salt-responsive, regenerative, double-layered polyzwitterionic brushes. *Chem. Eng. J.* **2018**, *333*, 1–10. [CrossRef]
30. Papayannopoulos, V. Neutrophil extracellular traps in immunity and disease. *Nat. Rev. Immunol.* **2018**, *18*, 134–147. [CrossRef] [PubMed]
31. Zhou, C.; Wu, Y.; Thappeta, K.R.V.; Subramanian, J.T.L.; Pranantyo, D.; Kang, E.-T.; Duan, H.; Kline, K.; Chan-Park, M.B. In Vivo Anti-Biofilm and Anti-Bacterial Non-Leachable Coating Thermally Polymerized on Cylindrical Catheter. *ACS Appl. Mater. Interfaces* **2017**, *9*, 36269–36280. [CrossRef]
32. Thakuria, R.; Nath, N.K.; Saha, B.K. The Nature and Applications of π–π Interactions: A Perspective. *Cryst. Growth Des.* **2019**, *19*, 523–528. [CrossRef]
33. Puertas-Bartolomé, M.; Benito-Garzón, L.; Fung, S.; Kohn, J.; Vázquez-Lasa, B.; San Román, J. Bioadhesive functional hydrogels: Controlled release of catechol species with antioxidant and antiinflammatory behavior. *Mater. Sci. Eng. C Mater. Biol. Appl.* **2019**, *105*, 110040. [CrossRef]
34. Li, L.; Wang, Y.; Liu, K.; Yang, L.; Zhang, B.; Luo, Q.; Luo, R.; Wang, Y. Nanoparticles-stacked superhydrophilic coating supported synergistic antimicrobial ability for enhanced wound healing. *Mater. Sci. Eng. C Mater. Biol. Appl.* **2022**, *132*, 112535. [CrossRef]
35. Cai, B.; Zou, Q.; Zuo, Y.; Mei, Q.; Ma, J.; Lin, L.; Chen, L.; Li, Y. Injectable Gel Constructs with Regenerative and Anti-Infective Dual Effects Based on Assembled Chitosan Microspheres. *ACS Appl. Mater. Interfaces* **2018**, *10*, 25099–25112. [CrossRef]
36. Han, L.; Wang, M.; Sun, H.; Li, P.; Wang, K.; Ren, F.; Lu, X. Porous titanium scaffolds with self-assembled micro/nano-hierarchical structure for dual functions of bone regeneration and anti-infection. *J. Biomed. Mater. Res. A* **2017**, *105*, 3482–3492. [CrossRef]
37. Yu, X.; Pan, Q.; Zheng, Z.; Chen, Y.; Chen, Y.; Weng, S.; Huang, L. pH-responsive and porous vancomycin-loaded PLGA microspheres: Evidence of controlled and sustained release for localized inflammation inhibition in vitro. *RSC Adv.* **2018**, *8*, 37424–37432. [CrossRef]
38. He, R.; Sui, J.; Wang, G.; Wang, Y.; Xu, K.; Qin, S.; Xu, S.; Ji, F.; Zhang, H. Polydopamine and hyaluronic acid immobilisation on vancomycin-loaded titanium nanotube for prophylaxis of implant infections. *Colloids Surf. B Biointerfaces* **2022**, *216*, 112582. [CrossRef] [PubMed]
39. Beck-Broichsitter, M.; Thieme, M.; Nguyen, J.; Schmehl, T.; Gessler, T.; Seeger, W.; Agarwal, S.; Greiner, A.; Kissel, T. Novel 'nano in nano' composites for sustained drug delivery: Biodegradable nanoparticles encapsulated into nanofiber non-wovens. *Macromol. Biosci.* **2010**, *10*, 1527–1535. [CrossRef] [PubMed]
40. Zhang, C.-L.; Yu, S.-H. Nanoparticles meet electrospinning: Recent advances and future prospects. *Chem. Soc. Rev.* **2014**, *43*, 4423–4448. [CrossRef] [PubMed]
41. Xue, J.; Niu, Y.; Gong, M.; Shi, R.; Chen, D.; Zhang, L.; Lvov, Y. Electrospun microfiber membranes embedded with drug-loaded clay nanotubes for sustained antimicrobial protection. *ACS Nano* **2015**, *9*, 1600–1612. [CrossRef]
42. Golda-Cepa, M.; Chorylek, A.; Chytrosz, P.; Brzychczy-Wloch, M.; Jaworska, J.; Kasperczyk, J.; Hakkarainen, M.; Engvall, K.; Kotarba, A. Multifunctional PLGA/Parylene C Coating for Implant Materials: An Integral Approach for Biointerface Optimization. *ACS Appl. Mater. Interfaces* **2016**, *8*, 22093–22105. [CrossRef] [PubMed]
43. Pan, P.; Yue, Q.; Li, J.; Gao, M.; Yang, X.; Ren, Y.; Cheng, X.; Cui, P.; Deng, Y. Smart Cargo Delivery System based on Mesoporous Nanoparticles for Bone Disease Diagnosis and Treatment. *Adv. Sci.* **2021**, *8*, e2004586. [CrossRef]

44. Tang, F.; Li, L.; Chen, D. Mesoporous silica nanoparticles: Synthesis, biocompatibility and drug delivery. *Adv. Mater.* **2012**, *24*, 1504–1534. [CrossRef]
45. Gao, X.; Li, L.; Cai, X.; Huang, Q.; Xiao, J.; Cheng, Y. Targeting nanoparticles for diagnosis and therapy of bone tumors: Opportunities and challenges. *Biomaterials* **2021**, *265*, 120404. [CrossRef]
46. Liu, Y.; Yu, P.; Peng, X.; Huang, Q.; Ding, M.; Chen, Y.; Jin, R.; Xie, J.; Zhao, C.; Li, J. Hexapeptide-conjugated calcitonin for targeted therapy of osteoporosis. *J. Control. Release* **2019**, *304*, 39–50. [CrossRef] [PubMed]
47. Chen, H.; Liu, C.; Chen, D.; Madrid, K.; Peng, S.; Dong, X.; Zhang, M.; Gu, Y. Bacteria-Targeting Conjugates Based on Antimicrobial Peptide for Bacteria Diagnosis and Therapy. *Mol. Pharm.* **2015**, *12*, 2505–2516. [CrossRef] [PubMed]
48. Nie, B.; Huo, S.; Qu, X.; Guo, J.; Liu, X.; Hong, Q.; Wang, Y.; Yang, J.; Yue, B. Bone infection site targeting nanoparticle-antibiotics delivery vehicle to enhance treatment efficacy of orthopedic implant related infection. *Bioact. Mater.* **2022**, *16*, 134–148. [CrossRef]
49. Kuang, Z.; Dai, G.; Wan, R.; Zhang, D.; Zhao, C.; Chen, C.; Li, J.; Gu, H.; Huang, W. Osteogenic and antibacterial dual functions of a novel levofloxacin loaded mesoporous silica microspheres/nano-hydroxyapatite/polyurethane composite scaffold. *Genes Dis.* **2021**, *8*, 193–202. [CrossRef]
50. Chou, S.-F.; Carson, D.; Woodrow, K.A. Current strategies for sustaining drug release from electrospun nanofibers. *J. Control. Release* **2015**, *220*, 584–591. [CrossRef]
51. Wang, Y.; Jiang, Y.; Zhang, Y.; Wen, S.; Wang, Y.; Zhang, H. Dual functional electrospun core-shell nanofibers for anti-infective guided bone regeneration membranes. *Mater. Sci. Eng. C Mater. Biol. Appl.* **2019**, *98*, 134–139. [CrossRef]
52. Ansari, N.; Lodha, A.; Menon, S.K. Smart platform for the time since death determination from vitreous humor cystine. *Biosens. Bioelectron.* **2016**, *86*, 115–121. [CrossRef]
53. Tanaka, M.; Saito, S.; Kita, R.; Jang, J.; Choi, Y.; Choi, J.; Okochi, M. Array-Based Screening of Silver Nanoparticle Mineralization Peptides. *Int. J. Mol. Sci.* **2020**, *21*, 2377. [CrossRef] [PubMed]
54. Granados, A.; Pleixats, R.; Vallribera, A. Recent Advances on Antimicrobial and Anti-Inflammatory Cotton Fabrics Containing Nanostructures. *Molecules* **2021**, *26*, 3008. [CrossRef] [PubMed]
55. Chae, K.; Jang, W.Y.; Park, K.; Lee, J.; Kim, H.; Lee, K.; Lee, C.K.; Lee, Y.; Lee, S.H.; Seo, J. Antibacterial infection and immune-evasive coating for orthopedic implants. *Sci. Adv.* **2020**, *6*, eabb0025. [CrossRef] [PubMed]
56. Lee, J.; Yoo, J.; Kim, J.; Jang, Y.; Shin, K.; Ha, E.; Ryu, S.; Kim, B.-G.; Wooh, S.; Char, K. Development of Multimodal Antibacterial Surfaces Using Porous Amine-Reactive Films Incorporating Lubricant and Silver Nanoparticles. *ACS Appl. Mater. Interfaces* **2019**, *11*, 6550–6560. [CrossRef]
57. Franci, G.; Falanga, A.; Galdiero, S.; Palomba, L.; Rai, M.; Morelli, G.; Galdiero, M. Silver nanoparticles as potential antibacterial agents. *Molecules* **2015**, *20*, 8856–8874. [CrossRef]
58. Chang, M.-H.; Hsiao, Y.-P.; Hsu, C.-Y.; Lai, P.-S. Photo-Crosslinked Polymeric Matrix with Antimicrobial Functions for Excisional Wound Healing in Mice. *Nanomaterials* **2018**, *8*, 791. [CrossRef]
59. Mohd Yusof, H.; Abdul Rahman, N.; Mohamad, R.; Zaidan, U.H.; Samsudin, A.A. Biosynthesis of zinc oxide nanoparticles by cell-biomass and supernatant of Lactobacillus plantarum TA4 and its antibacterial and biocompatibility properties. *Sci. Rep.* **2020**, *10*, 19996. [CrossRef] [PubMed]
60. Lipovsky, A.; Nitzan, Y.; Gedanken, A.; Lubart, R. Antifungal activity of ZnO nanoparticles—The role of ROS mediated cell injury. *Nanotechnology* **2011**, *22*, 105101. [CrossRef]
61. Shi, M.; Kwon, H.S.; Peng, Z.; Elder, A.; Yang, H. Effects of surface chemistry on the generation of reactive oxygen species by copper nanoparticles. *ACS Nano* **2012**, *6*, 2157–2164. [CrossRef]
62. Chang, Y.-N.; Zhang, M.; Xia, L.; Zhang, J.; Xing, G. The Toxic Effects and Mechanisms of CuO and ZnO Nanoparticles. *Materials* **2012**, *5*, 2850–2871. [CrossRef]
63. Dayaghi, E.; Bakhsheshi-Rad, H.R.; Hamzah, E.; Akhavan-Farid, A.; Ismail, A.F.; Aziz, M.; Abdolahi, E. Magnesium-zinc scaffold loaded with tetracycline for tissue engineering application: In vitro cell biology and antibacterial activity assessment. *Mater. Sci. Eng. C Mater. Biol. Appl.* **2019**, *102*, 53–65. [CrossRef]
64. Coelho, C.C.; Padrão, T.; Costa, L.; Pinto, M.T.; Costa, P.C.; Domingues, V.F.; Quadros, P.A.; Monteiro, F.J.; Sousa, S.R. The antibacterial and angiogenic effect of magnesium oxide in a hydroxyapatite bone substitute. *Sci. Rep.* **2020**, *10*, 19098. [CrossRef] [PubMed]
65. Shuai, C.; Dong, Z.; He, C.; Yang, W.; Peng, S.; Yang, Y.; Qi, F. A peritectic phase refines the microstructure and enhances Zn implants. *J. Mater. Res. Technol.* **2020**, *9*, 2623–2634. [CrossRef]
66. Sui, J.; Liu, S.; Chen, M.; Zhang, H. Surface Bio-Functionalization of Anti-Bacterial Titanium Implants: A Review. *Coatings* **2022**, *12*, 1125. [CrossRef]
67. Auger, S.; Henry, C.; Péchoux, C.; Suman, S.; Lejal, N.; Bertho, N.; Larcher, T.; Stankic, S.; Vidic, J. Exploring multiple effects of $Zn_{0.15}Mg_{0.85}O$ nanoparticles on Bacillus subtilis and macrophages. *Sci. Rep.* **2018**, *8*, 12276. [CrossRef] [PubMed]
68. Santiago-Castillo, K.; Torres-Huerta, A.M.; Del Ángel-López, D.; Domínguez-Crespo, M.A.; Dorantes-Rosales, H.; Palma-Ramírez, D.; Willcock, H. In Situ Growth of Silver Nanoparticles on Chitosan Matrix for the Synthesis of Hybrid Electrospun Fibers: Analysis of Microstructural and Mechanical Properties. *Polymers* **2022**, *14*, 674. [CrossRef]
69. Ghasemian Lemraski, E.; Jahangirian, H.; Dashti, M.; Khajehali, E.; Sharafinia, S.; Rafiee-Moghaddam, R.; Webster, T.J. Antimicrobial Double-Layer Wound Dressing Based on Chitosan/Polyvinyl Alcohol/Copper: In vitro and in vivo Assessment. *Int. J. Nanomed.* **2021**, *16*, 223–235. [CrossRef]

70. Bandeira, M.; Chee, B.S.; Frassini, R.; Nugent, M.; Giovanela, M.; Roesch-Ely, M.; Da Crespo, J.S.; Devine, D.M. Antimicrobial PAA/PAH Electrospun Fiber Containing Green Synthesized Zinc Oxide Nanoparticles for Wound Healing. *Materials* **2021**, *14*, 2889. [CrossRef]
71. Jia, Z.; Xiu, P.; Xiong, P.; Zhou, W.; Cheng, Y.; Wei, S.; Zheng, Y.; Xi, T.; Cai, H.; Liu, Z.; et al. Additively Manufactured Macroporous Titanium with Silver-Releasing Micro-/Nanoporous Surface for Multipurpose Infection Control and Bone Repair—A Proof of Concept. *ACS Appl. Mater. Interfaces* **2016**, *8*, 28495–28510. [CrossRef]
72. Antezana, P.E.; Municoy, S.; Pérez, C.J.; Desimone, M.F. Collagen Hydrogels Loaded with Silver Nanoparticles and Cannabis Sativa Oil. *Antibiotics* **2021**, *10*, 1420. [CrossRef]
73. Gao, F.; Shao, T.; Yu, Y.; Xiong, Y.; Yang, L. Surface-bound reactive oxygen species generating nanozymes for selective antibacterial action. *Nat. Commun.* **2021**, *12*, 745. [CrossRef]
74. Lu, Z.; Rong, K.; Li, J.; Yang, H.; Chen, R. Size-dependent antibacterial activities of silver nanoparticles against oral anaerobic pathogenic bacteria. *J. Mater. Sci. Mater. Med.* **2013**, *24*, 1465–1471. [CrossRef]
75. Xue, C.; Song, X.; Liu, M.; Ai, F.; Liu, M.; Shang, Q.; Shi, X.; Li, F.; He, X.; Xie, L.; et al. A highly efficient, low-toxic, wide-spectrum antibacterial coating designed for 3D printed implants with tailorable release properties. *J. Mater. Chem. B* **2017**, *5*, 4128–4136. [CrossRef]
76. Sharma, V.K.; Yngard, R.A.; Lin, Y. Silver nanoparticles: Green synthesis and their antimicrobial activities. *Adv. Colloid Interface Sci.* **2009**, *145*, 83–96. [CrossRef] [PubMed]
77. Sun, H.; Lv, L.; Bai, Y.; Yang, H.; Zhou, H.; Li, C.; Yang, L. Nanotechnology-enabled materials for hemostatic and anti-infection treatments in orthopedic surgery. *Int. J. Nanomed.* **2018**, *13*, 8325–8338. [CrossRef] [PubMed]
78. Le Ouay, B.; Stellacci, F. Antibacterial activity of silver nanoparticles: A surface science insight. *Nano Today* **2015**, *10*, 339–354. [CrossRef]
79. Morones-Ramirez, J.R.; Winkler, J.A.; Spina, C.S.; Collins, J.J. Silver enhances antibiotic activity against gram-negative bacteria. *Sci. Transl. Med.* **2013**, *5*, 190ra81. [CrossRef]
80. Shang, H.; Zhou, Z.; Wu, X.; Li, X.; Xu, Y. Sunlight-Induced Synthesis of Non-Target Biosafety Silver Nanoparticles for the Control of Rice Bacterial Diseases. *Nanomaterials* **2020**, *10*, 2007. [CrossRef] [PubMed]
81. Cao, H.; Qiao, Y.; Meng, F.; Liu, X. Spacing-Dependent Antimicrobial Efficacy of Immobilized Silver Nanoparticles. *J. Phys. Chem. Lett.* **2014**, *5*, 743–748. [CrossRef] [PubMed]
82. Sagliocchi, S.; Cicatiello, A.G.; Di Cicco, E.; Ambrosio, R.; Miro, C.; Di Girolamo, D.; Nappi, A.; Mancino, G.; de Stefano, M.A.; Luongo, C.; et al. The thyroid hormone activating enzyme, type 2 deiodinase, induces myogenic differentiation by regulating mitochondrial metabolism and reducing oxidative stress. *Redox Biol.* **2019**, *24*, 101228. [CrossRef] [PubMed]
83. Jiménez-Holguín, J.; Sánchez-Salcedo, S.; Cicuéndez, M.; Vallet-Regí, M.; Salinas, A.J. Cu-Doped Hollow Bioactive Glass Nanoparticles for Bone Infection Treatment. *Pharmaceutics* **2022**, *14*, 845. [CrossRef] [PubMed]
84. Yeroslavsky, G.; Lavi, R.; Alishaev, A.; Rahimipour, S. Sonochemically-Produced Metal-Containing Polydopamine Nanoparticles and Their Antibacterial and Antibiofilm Activity. *Langmuir* **2016**, *32*, 5201–5212. [CrossRef] [PubMed]
85. Baker, J.; Sitthisak, S.; Sengupta, M.; Johnson, M.; Jayaswal, R.K.; Morrissey, J.A. Copper stress induces a global stress response in *Staphylococcus aureus* and represses *sae* and *agr* expression and biofilm formation. *Appl. Environ. Microbiol.* **2010**, *76*, 150–160. [CrossRef] [PubMed]
86. Maertens, L.; Coninx, I.; Claesen, J.; Leys, N.; Matroule, J.-Y.; van Houdt, R. Copper Resistance Mediates Long-Term Survival of *Cupriavidus metallidurans* in Wet Contact with Metallic Copper. *Front. Microbiol.* **2020**, *11*, 1208. [CrossRef] [PubMed]
87. Xiu, W.; Wan, L.; Yang, K.; Li, X.; Yuwen, L.; Dong, H.; Mou, Y.; Yang, D.; Wang, L. Potentiating hypoxic microenvironment for antibiotic activation by photodynamic therapy to combat bacterial biofilm infections. *Nat. Commun.* **2022**, *13*, 3875. [CrossRef]
88. Li, Z.; Xie, K.; Yang, S.; Yu, T.; Xiao, Y.; Zhou, Y. Multifunctional Ca-Zn-Si-based micro-nano spheres with anti-infective, anti-inflammatory, and dentin regenerative properties for pulp capping application. *J. Mater. Chem. B* **2021**, *9*, 8289–8299. [CrossRef]
89. Dediu, V.; Busila, M.; Tucureanu, V.; Bucur, F.I.; Iliescu, F.S.; Brincoveanu, O.; Iliescu, C. Synthesis of ZnO/Au Nanocomposite for Antibacterial Applications. *Nanomaterials* **2022**, *12*, 3832. [CrossRef]
90. Dwivedi, S.; Wahab, R.; Khan, F.; Mishra, Y.K.; Musarrat, J.; Al-Khedhairy, A.A. Reactive oxygen species mediated bacterial biofilm inhibition via zinc oxide nanoparticles and their statistical determination. *PLoS ONE* **2014**, *9*, e111289. [CrossRef]
91. Kumar, R.; Umar, A.; Kumar, G.; Nalwa, H.S. Antimicrobial properties of ZnO nanomaterials: A review. *Ceram. Int.* **2017**, *43*, 3940–3961. [CrossRef]
92. Mishra, P.K.; Mishra, H.; Ekielski, A.; Talegaonkar, S.; Vaidya, B. Zinc oxide nanoparticles: A promising nanomaterial for biomedical applications. *Drug Discov. Today* **2017**, *22*, 1825–1834. [CrossRef]
93. Jalil, S.A.; Akram, M.; Bhat, J.A.; Hayes, J.J.; Singh, S.C.; ElKabbash, M.; Guo, C. Creating superhydrophobic and antibacterial surfaces on gold by femtosecond laser pulses. *Appl. Surf. Sci.* **2020**, *506*, 144952. [CrossRef]
94. Regiel-Futyra, A.; Kus-Liśkiewicz, M.; Sebastian, V.; Irusta, S.; Arruebo, M.; Stochel, G.; Kyzioł, A. Development of noncytotoxic chitosan-gold nanocomposites as efficient antibacterial materials. *ACS Appl. Mater. Interfaces* **2015**, *7*, 1087–1099. [CrossRef] [PubMed]
95. Ren, F.; Yesildag, C.; Zhang, Z.; Lensen, M.C. Surface Patterning of Gold Nanoparticles on PEG-Based Hydrogels to Control Cell Adhesion. *Polymers* **2017**, *9*, 154. [CrossRef]

96. Tamayo, L.; Acuña, D.; Riveros, A.L.; Kogan, M.J.; Azócar, M.I.; Páez, M.; Leal, M.; Urzúa, M.; Cerda, E. Porous Nanogold/Polyurethane Scaffolds with Improved Antibiofilm, Mechanical, and Thermal Properties and with Reduced Effects on Cell Viability: A Suitable Material for Soft Tissue Applications. *ACS Appl. Mater. Interfaces* **2018**, *10*, 13361–13372. [CrossRef] [PubMed]
97. Cui, Y.; Zhao, Y.; Tian, Y.; Zhang, W.; Lü, X.; Jiang, X. The molecular mechanism of action of bactericidal gold nanoparticles on Escherichia coli. *Biomaterials* **2012**, *33*, 2327–2333. [CrossRef]
98. Shareena Dasari, T.P.; Zhang, Y.; Yu, H. Antibacterial Activity and Cytotoxicity of Gold (I) and (III) Ions and Gold Nanoparticles. *Biochem. Pharmacol.* **2015**, *4*, 199. [CrossRef]
99. Ali, D.; Alarifi, S.; Alkahtani, S.; Almeer, R.S. Silver-doped graphene oxide nanocomposite triggers cytotoxicity and apoptosis in human hepatic normal and carcinoma cells. *Int. J. Nanomed.* **2018**, *13*, 5685–5699. [CrossRef]
100. Pohanka, M. Copper and copper nanoparticles toxicity and their impact on basic functions in the body. *Bratisl. Lek. Listy* **2019**, *120*, 397–409. [CrossRef]
101. Malhotra, N.; Ger, T.-R.; Uapipatanakul, B.; Huang, J.-C.; Chen, K.H.-C.; Hsiao, C.-D. Review of Copper and Copper Nanoparticle Toxicity in Fish. *Nanomaterials* **2020**, *10*, 1126. [CrossRef]
102. Canta, M.; Cauda, V. The investigation of the parameters affecting the ZnO nanoparticle cytotoxicity behaviour: A tutorial review. *Biomater. Sci.* **2020**, *8*, 6157–6174. [CrossRef]
103. d'Amora, M.; Schmidt, T.J.N.; Konstantinidou, S.; Raffa, V.; de Angelis, F.; Tantussi, F. Effects of Metal Oxide Nanoparticles in Zebrafish. *Oxid. Med. Cell. Longev.* **2022**, *2022*, 3313016. [CrossRef] [PubMed]
104. Sani, A.; Cao, C.; Cui, D. Toxicity of gold nanoparticles (AuNPs): A review. *Biochem. Biophys. Rep.* **2021**, *26*, 100991. [CrossRef]
105. Sonavane, G.; Tomoda, K.; Sano, A.; Ohshima, H.; Terada, H.; Makino, K. In vitro permeation of gold nanoparticles through rat skin and rat intestine: Effect of particle size. *Colloids Surf. B Biointerfaces* **2008**, *65*, 1–10. [CrossRef]
106. Mellor, R.D.; Uchegbu, I.F. Ultrasmall-in-Nano: Why Size Matters. *Nanomaterials* **2022**, *12*, 2467. [CrossRef] [PubMed]
107. Wang, J.-Y.; Chen, J.; Yang, J.; Wang, H.; Shen, X.; Sun, Y.-M.; Guo, M.; Zhang, X.-D. Effects of surface charges of gold nanoclusters on long-term in vivo biodistribution, toxicity, and cancer radiation therapy. *Int. J. Nanomed.* **2016**, *11*, 3475–3485. [CrossRef]
108. Alavi, M.; Nokhodchi, A. An overview on antimicrobial and wound healing properties of ZnO nanobiofilms, hydrogels, and bionanocomposites based on cellulose, chitosan, and alginate polymers. *Carbohydr. Polym.* **2020**, *227*, 115349. [CrossRef] [PubMed]
109. Nava, O.J.; Soto-Robles, C.A.; Gómez-Gutiérrez, C.M.; Vilchis-Nestor, A.R.; Castro-Beltrán, A.; Olivas, A.; Luque, P.A. Fruit peel extract mediated green synthesis of zinc oxide nanoparticles. *J. Mol. Struct.* **2017**, *1147*, 1–6. [CrossRef]
110. Zhang, Q.; Zhang, H.; Hui, A.; Ding, J.; Liu, X.; Wang, A. Synergistic Effect of Glycyrrhizic Acid and ZnO/Palygorskite on Improving Chitosan-Based Films and Their Potential Application in Wound Healing. *Polymers* **2021**, *13*, 3878. [CrossRef]
111. Kalemtas, A.; Kocer, H.B.; Aydin, A.; Terzioglu, P.; Aydin, G. Mechanical and antibacterial properties of ZnO/chitosan biocomposite films. *J. Polym. Eng.* **2022**, *42*, 35–47. [CrossRef]
112. Hasanin, M.; Swielam, E.M.; Atwa, N.A.; Agwa, M.M. Novel design of bandages using cotton pads, doped with chitosan, glycogen and ZnO nanoparticles, having enhanced antimicrobial and wounds healing effects. *Int. J. Biol. Macromol.* **2022**, *197*, 121–130. [CrossRef]
113. Joorabloo, A.; Khorasani, M.T.; Adeli, H.; Brouki Milan, P.; Amoupour, M. Using artificial neural network for design and development of PVA/chitosan/starch/heparinized nZnO hydrogels for enhanced wound healing. *J. Ind. Eng. Chem.* **2022**, *108*, 88–100. [CrossRef]
114. Keerthana, S.; Kumar, A. Potential risks and benefits of zinc oxide nanoparticles: A systematic review. *Crit. Rev. Toxicol.* **2020**, *50*, 47–71. [CrossRef] [PubMed]
115. Chen, F.-C.; Huang, C.-M.; Yu, X.-W.; Chen, Y.-Y. Effect of nano zinc oxide on proliferation and toxicity of human gingival cells. *Hum. Exp. Toxicol.* **2022**, *41*, 9603271221080236. [CrossRef] [PubMed]
116. Zeghoud, S.; Hemmami, H.; Ben Seghir, B.; Ben Amor, I.; Kouadri, I.; Rebiai, A.; Messaoudi, M.; Ahmed, S.; Pohl, P.; Simal-Gandara, J. A review on biogenic green synthesis of ZnO nanoparticles by plant biomass and their applications. *Mater. Today Commun.* **2022**, *33*, 104747. [CrossRef]
117. Karuppannan, S.K.; Ramalingam, R.; Mohamed Khalith, S.B.; Musthafa, S.A.; Dowlath, M.J.H.; Munuswamy-Ramanujam, G.; Arunachalam, K.D. Copper oxide nanoparticles infused electrospun polycaprolactone/gelatin scaffold as an antibacterial wound dressing. *Mater. Lett.* **2021**, *294*, 129787. [CrossRef]
118. Raba-Páez, A.M.; D Malafatti, J.O.; Parra-Vargas, C.A.; Paris, E.C.; Rincón-Joya, M. Effect of tungsten doping on the structural, morphological and bactericidal properties of nanostructured CuO. *PLoS ONE* **2020**, *15*, e0239868. [CrossRef]
119. Cheng, T.-M.; Chu, H.-Y.; Huang, H.-M.; Li, Z.-L.; Chen, C.-Y.; Shih, Y.-J.; Whang-Peng, J.; Cheng, R.H.; Mo, J.-K.; Lin, H.-Y.; et al. Toxicologic Concerns with Current Medical Nanoparticles. *Int. J. Mol. Sci.* **2022**, *23*, 7597. [CrossRef] [PubMed]
120. Yudaev, P.; Mezhuev, Y.; Chistyakov, E. Nanoparticle-Containing Wound Dressing: Antimicrobial and Healing Effects. *Gels* **2022**, *8*, 329. [CrossRef]
121. Alarifi, S.; Ali, D.; Verma, A.; Alakhtani, S.; Ali, B.A. Cytotoxicity and genotoxicity of copper oxide nanoparticles in human skin keratinocytes cells. *Int. J. Toxicol.* **2013**, *32*, 296–307. [CrossRef] [PubMed]
122. Mahapatra, O.; Bhagat, M.; Gopalakrishnan, C.; Arunachalam, K.D. Ultrafine dispersed CuO nanoparticles and their antibacterial activity. *J. Exp. Nanosci.* **2008**, *3*, 185–193. [CrossRef]

123. Mersian, H.; Alizadeh, M.; Hadi, N. Synthesis of zirconium doped copper oxide (CuO) nanoparticles by the Pechini route and investigation of their structural and antibacterial properties. *Ceram. Int.* **2018**, *44*, 20399–20408. [CrossRef]
124. Thakur, N.; Anu; Kumar, K. Effect of (Ag, Co) co-doping on the structural and antibacterial efficiency of CuO nanoparticles: A rapid microwave assisted method. *J. Environ. Chem. Eng.* **2020**, *8*, 104011. [CrossRef]
125. Kumar, P.; Chandra Mathpal, M.; Prakash, J.; Viljoen, B.C.; Roos, W.D.; Swart, H.C. Band gap tailoring of cauliflower-shaped CuO nanostructures by Zn doping for antibacterial applications. *J. Alloys Compd.* **2020**, *832*, 154968. [CrossRef]
126. Pop, O.L.; Mesaros, A.; Vodnar, D.C.; Suharoschi, R.; Tăbăran, F.; Mageruşan, L.; Tódor, I.S.; Diaconeasa, Z.; Balint, A.; Ciontea, L.; et al. Cerium Oxide Nanoparticles and Their Efficient Antibacterial Application In Vitro against Gram-Positive and Gram-Negative Pathogens. *Nanomaterials* **2020**, *10*, 1614. [CrossRef]
127. Zamani, K.; Allah-Bakhshi, N.; Akhavan, F.; Yousefi, M.; Golmoradi, R.; Ramezani, M.; Bach, H.; Razavi, S.; Irajian, G.-R.; Gerami, M.; et al. Antibacterial effect of cerium oxide nanoparticle against *Pseudomonas aeruginosa*. *BMC Biotechnol.* **2021**, *21*, 68. [CrossRef]
128. Qi, M.; Li, W.; Zheng, X.; Li, X.; Sun, Y.; Wang, Y.; Li, C.; Wang, L. Cerium and Its Oxidant-Based Nanomaterials for Antibacterial Applications: A State-of-the-Art Review. *Front. Mater.* **2020**, *7*, 213. [CrossRef]
129. Abdal Dayem, A.; Hossain, M.K.; Lee, S.B.; Kim, K.; Saha, S.K.; Yang, G.-M.; Choi, H.Y.; Cho, S.-G. The Role of Reactive Oxygen Species (ROS) in the Biological Activities of Metallic Nanoparticles. *Int. J. Mol. Sci.* **2017**, *18*, 120. [CrossRef] [PubMed]
130. David, M.E.; Ion, R.M.; Grigorescu, R.M.; Iancu, L.; Holban, A.M.; Iordache, F.; Nicoara, A.I.; Alexandrescu, E.; Somoghi, R.; Teodorescu, S.; et al. Biocompatible and Antimicrobial Cellulose Acetate-Collagen Films Containing MWCNTs Decorated with TiO_2 Nanoparticles for Potential Biomedical Applications. *Nanomaterials* **2022**, *12*, 239. [CrossRef] [PubMed]
131. Shang, C.; Bu, J.; Song, C. Preparation, Antimicrobial Properties under Different Light Sources, Mechanisms and Applications of TiO_2: A Review. *Materials* **2022**, *15*, 5820. [CrossRef] [PubMed]
132. Hossain, M.M.; Polash, S.A.; Takikawa, M.; Shubhra, R.D.; Saha, T.; Islam, Z.; Hossain, S.; Hasan, M.A.; Takeoka, S.; Sarker, S.R. Investigation of the Antibacterial Activity and in vivo Cytotoxicity of Biogenic Silver Nanoparticles as Potent Therapeutics. *Front. Bioeng. Biotechnol.* **2019**, *7*, 239. [CrossRef] [PubMed]
133. Niloy, M.S.; Hossain, M.M.; Takikawa, M.; Shakil, M.S.; Polash, S.A.; Mahmud, K.M.; Uddin, M.F.; Alam, M.; Shubhra, R.D.; Shawan, M.M.A.K.; et al. Synthesis of Biogenic Silver Nanoparticles Using Caesalpinia digyna and Investigation of Their Antimicrobial Activity and In Vivo Biocompatibility. *ACS Appl. Bio Mater.* **2020**, *3*, 7722–7733. [CrossRef] [PubMed]
134. Yan, B.; Ai, Y.; Sun, Q.; Ma, Y.; Cao, Y.; Wang, J.; Zhang, Z.; Wang, X. Membrane Damage during Ferroptosis Is Caused by Oxidation of Phospholipids Catalyzed by the Oxidoreductases POR and CYB5R1. *Mol. Cell* **2021**, *81*, 355–369.e10. [CrossRef]
135. Collin, F. Chemical Basis of Reactive Oxygen Species Reactivity and Involvement in Neurodegenerative Diseases. *Int. J. Mol. Sci.* **2019**, *20*, 2407. [CrossRef]
136. Yougbaré, S.; Mutalik, C.; Okoro, G.; Lin, I.-H.; Krisnawati, D.I.; Jazidie, A.; Nuh, M.; Chang, C.-C.; Kuo, T.-R. Emerging Trends in Nanomaterials for Antibacterial Applications. *Int. J. Nanomed.* **2021**, *16*, 5831–5867. [CrossRef]
137. Li, K.; Chen, Y.; Zhang, W.; Pu, Z.; Jiang, L.; Chen, Y. Surface interactions affect the toxicity of engineered metal oxide nanoparticles toward Paramecium. *Chem. Res. Toxicol.* **2012**, *25*, 1675–1681. [CrossRef]
138. Li, J.; Wang, J.; Wang, D.; Guo, G.; Yeung, K.W.K.; Zhang, X.; Liu, X. Band Gap Engineering of Titania Film through Cobalt Regulation for Oxidative Damage of Bacterial Respiration and Viability. *ACS Appl. Mater. Interfaces* **2017**, *9*, 27475–27490. [CrossRef]
139. Franco, D.; Calabrese, G.; Guglielmino, S.P.P.; Conoci, S. Metal-Based Nanoparticles: Antibacterial Mechanisms and Biomedical Application. *Microorganisms* **2022**, *10*, 1778. [CrossRef]
140. Vahdati, M.; Tohidi Moghadam, T. Synthesis and Characterization of Selenium Nanoparticles-Lysozyme Nanohybrid System with Synergistic Antibacterial Properties. *Sci. Rep.* **2020**, *10*, 510. [CrossRef]
141. Truong, L.B.; Medina-Cruz, D.; Mostafavi, E.; Rabiee, N. Selenium Nanomaterials to Combat Antimicrobial Resistance. *Molecules* **2021**, *26*, 3611. [CrossRef]
142. Bano, I.; Skalickova, S.; Arbab, S.; Urbankova, L.; Horky, P. Toxicological effects of nanoselenium in animals. *J. Anim. Sci. Biotechnol.* **2022**, *13*, 72. [CrossRef]
143. Biswas, D.P.; O'Brien-Simpson, N.M.; Reynolds, E.C.; O'Connor, A.J.; Tran, P.A. Comparative study of novel in situ decorated porous chitosan-selenium scaffolds and porous chitosan-silver scaffolds towards antimicrobial wound dressing application. *J. Colloid Interface Sci.* **2018**, *515*, 78–91. [CrossRef] [PubMed]
144. Shakibaie, M.; Forootanfar, H.; Golkari, Y.; Mohammadi-Khorsand, T.; Shakibaie, M.R. Anti-biofilm activity of biogenic selenium nanoparticles and selenium dioxide against clinical isolates of *Staphylococcus aureus*, *Pseudomonas aeruginosa*, and *Proteus mirabilis*. *J. Trace Elem. Med. Biol.* **2015**, *29*, 235–241. [CrossRef] [PubMed]
145. Tran, P.A.; O'Brien-Simpson, N.; Palmer, J.A.; Bock, N.; Reynolds, E.C.; Webster, T.J.; Deva, A.; Morrison, W.A.; O'Connor, A.J. Selenium nanoparticles as anti-infective implant coatings for trauma orthopedics against methicillin-resistant *Staphylococcus aureus* and epidermidis: In vitro and in vivo assessment. *Int. J. Nanomed.* **2019**, *14*, 4613–4624. [CrossRef] [PubMed]
146. Chen, W.; Cheng, H.; Xia, W. Progress in the Surface Functionalization of Selenium Nanoparticles and Their Potential Application in Cancer Therapy. *Antioxidants* **2022**, *11*, 1965. [CrossRef] [PubMed]
147. Shakibaie, M.; Shahverdi, A.R.; Faramarzi, M.A.; Hassanzadeh, G.R.; Rahimi, H.R.; Sabzevari, O. Acute and subacute toxicity of novel biogenic selenium nanoparticles in mice. *Pharm. Biol.* **2013**, *51*, 58–63. [CrossRef]

148. Tran, P.A.; O'Brien-Simpson, N.; Reynolds, E.C.; Pantarat, N.; Biswas, D.P.; O'Connor, A.J. Low cytotoxic trace element selenium nanoparticles and their differential antimicrobial properties against *S. aureus* and *E. coli*. *Nanotechnology* **2016**, *27*, 45101. [CrossRef]
149. Liang, X.; Zhang, S.; Gadd, G.M.; McGrath, J.; Rooney, D.W.; Zhao, Q. Fungal-derived selenium nanoparticles and their potential applications in electroless silver coatings for preventing pin-tract infections. *Regen. Biomater.* **2022**, *9*, rbac013. [CrossRef]
150. Guo, G.; Zhou, H.; Wang, Q.; Wang, J.; Tan, J.; Li, J.; Jin, P.; Shen, H. Nano-layered magnesium fluoride reservoirs on biomaterial surfaces strengthen polymorphonuclear leukocyte resistance to bacterial pathogens. *Nanoscale* **2017**, *9*, 875–892. [CrossRef]
151. Pramoda Kumari, J. Fluoride and Its Interaction with Human Life—A Review. *Word J. Pharm. Res.* **2017**, *6*, 292–315. [CrossRef]
152. Voyich, J.M.; Braughton, K.R.; Sturdevant, D.E.; Whitney, A.R.; Saïd-Salim, B.; Porcella, S.F.; Long, R.D.; Dorward, D.W.; Gardner, D.J.; Kreiswirth, B.N.; et al. Insights into mechanisms used by *Staphylococcus aureus* to avoid destruction by human neutrophils. *J. Immunol.* **2005**, *175*, 3907–3919. [CrossRef] [PubMed]
153. Breaker, R.R. New insight on the response of bacteria to fluoride. *Caries Res.* **2012**, *46*, 78–81. [CrossRef]
154. Zheng, T.-X.; Li, W.; Gu, Y.-Y.; Zhao, D.; Qi, M.-C. Classification and research progress of implant surface antimicrobial techniques. *J. Dent. Sci.* **2022**, *17*, 1–7. [CrossRef]
155. Gentleman, E.; Stevens, M.M.; Hill, R.G.; Brauer, D.S. Surface properties and ion release from fluoride-containing bioactive glasses promote osteoblast differentiation and mineralization in vitro. *Acta Biomater.* **2013**, *9*, 5771–5779. [CrossRef]
156. Wang, L.; He, S.; Wu, X.; Liang, S.; Mu, Z.; Wei, J.; Deng, F.; Deng, Y.; Wei, S. Polyetheretherketone/nano-fluorohydroxyapatite composite with antimicrobial activity and osseointegration properties. *Biomaterials* **2014**, *35*, 6758–6775. [CrossRef] [PubMed]
157. Lellouche, J.; Friedman, A.; Lellouche, J.-P.; Gedanken, A.; Banin, E. Improved antibacterial and antibiofilm activity of magnesium fluoride nanoparticles obtained by water-based ultrasound chemistry. *Nanomedicine* **2012**, *8*, 702–711. [CrossRef]
158. Ahmad, Z.; Senior, A.E. Inhibition of the ATPase activity of Escherichia coli ATP synthase by magnesium fluoride. *FEBS Lett.* **2006**, *580*, 517–520. [CrossRef]
159. Lellouche, J.; Friedman, A.; Gedanken, A.; Banin, E. Antibacterial and antibiofilm properties of yttrium fluoride nanoparticles. *Int. J. Nanomed.* **2012**, *7*, 5611–5624. [CrossRef]
160. Koyappayil, A.; Chavan, S.G.; Roh, Y.-G.; Lee, M.-H. Advances of MXenes; Perspectives on Biomedical Research. *Biosensors* **2022**, *12*, 454. [CrossRef]
161. Lin, H.; Wang, Y.; Gao, S.; Chen, Y.; Shi, J. Theranostic 2D Tantalum Carbide (MXene). *Adv. Mater.* **2018**, *30*, 1703284. [CrossRef]
162. Dai, C.; Chen, Y.; Jing, X.; Xiang, L.; Yang, D.; Lin, H.; Liu, Z.; Han, X.; Wu, R. Two-Dimensional Tantalum Carbide (MXenes) Composite Nanosheets for Multiple Imaging-Guided Photothermal Tumor Ablation. *ACS Nano* **2017**, *11*, 12696–12712. [CrossRef]
163. Rasool, K.; Helal, M.; Ali, A.; Ren, C.E.; Gogotsi, Y.; Mahmoud, K.A. Antibacterial Activity of Ti_3C_2Tx MXene. *ACS Nano* **2016**, *10*, 3674–3684. [CrossRef]
164. Yang, C.; Luo, Y.; Lin, H.; Ge, M.; Shi, J.; Zhang, X. Niobium Carbide MXene Augmented Medical Implant Elicits Bacterial Infection Elimination and Tissue Regeneration. *ACS Nano* **2021**, *15*, 1086–1099. [CrossRef]
165. Thoendel, M.; Kavanaugh, J.S.; Flack, C.E.; Horswill, A.R. Peptide signaling in the staphylococci. *Chem. Rev.* **2011**, *111*, 117–151. [CrossRef]
166. García-Betancur, J.-C.; Goñi-Moreno, A.; Horger, T.; Schott, M.; Sharan, M.; Eikmeier, J.; Wohlmuth, B.; Zernecke, A.; Ohlsen, K.; Kuttler, C.; et al. Cell differentiation defines acute and chronic infection cell types in *Staphylococcus aureus*. *Elife* **2017**, *6*, e28023. [CrossRef]
167. Arabi Shamsabadi, A.; Sharifian Gh, M.; Anasori, B.; Soroush, M. Antimicrobial Mode-of-Action of Colloidal Ti_3C_2Tx MXene Nanosheets. *ACS Sustain. Chem. Eng.* **2018**, *6*, 16586–16596. [CrossRef]
168. Kang, K.-T.; Koh, Y.-G.; Son, J.; Yeom, J.S.; Park, J.-H.; Kim, H.-J. Biomechanical evaluation of pedicle screw fixation system in spinal adjacent levels using polyetheretherketone, carbon-fiber-reinforced polyetheretherketone, and traditional titanium as rod materials. *Compos. Part B Eng.* **2017**, *130*, 248–256. [CrossRef]
169. Tang, X.; Dai, J.; Sun, H.; Nabanita, S.; Petr, S.; Wang, D.; Cheng, Q.; Wei, J. Mechanical Strength, Surface Properties, Cytocompatibility and Antibacterial Activity of Nano Zinc-Magnesium Silicate/Polyetheretherketone Biocomposites. *J. Nanosci. Nanotechnol.* **2019**, *19*, 7615–7623. [CrossRef] [PubMed]
170. Ferraris, S.; Spriano, S. Antibacterial titanium surfaces for medical implants. *Mater. Sci. Eng. C Mater. Biol. Appl.* **2016**, *61*, 965–978. [CrossRef] [PubMed]
171. Jin, G.; Qin, H.; Cao, H.; Qian, S.; Zhao, Y.; Peng, X.; Zhang, X.; Liu, X.; Chu, P.K. Synergistic effects of dual Zn/Ag ion implantation in osteogenic activity and antibacterial ability of titanium. *Biomaterials* **2014**, *35*, 7699–7713. [CrossRef]
172. Wang, Y.-W.; Cao, A.; Jiang, Y.; Zhang, X.; Liu, J.-H.; Liu, Y.; Wang, H. Superior antibacterial activity of zinc oxide/graphene oxide composites originating from high zinc concentration localized around bacteria. *ACS Appl. Mater. Interfaces* **2014**, *6*, 2791–2798. [CrossRef]
173. Ergene, C.; Yasuhara, K.; Palermo, E.F. Biomimetic antimicrobial polymers: Recent advances in molecular design. *Polym. Chem.* **2018**, *9*, 2407–2427. [CrossRef]
174. Dai, Y.; Zhang, X.; Xia, F. Macromol. Rapid Commun. 19/2017. *Macromol. Rapid Commun.* **2017**, *38*. [CrossRef]
175. Chin, W.; Yang, C.; Ng, V.W.L.; Huang, Y.; Cheng, J.; Tong, Y.W.; Coady, D.J.; Fan, W.; Hedrick, J.L.; Yang, Y.Y. Biodegradable Broad-Spectrum Antimicrobial Polycarbonates: Investigating the Role of Chemical Structure on Activity and Selectivity. *Macromolecules* **2013**, *46*, 8797–8807. [CrossRef]

176. Lin, D.; Huang, Y.; Jiang, Q.; Zhang, W.; Yue, X.; Guo, S.; Xiao, P.; Du, Q.; Xing, J.; Deng, L.; et al. Structural contributions of blocked or grafted poly(2-dimethylaminoethyl methacrylate) on PEGylated polycaprolactone nanoparticles in siRNA delivery. *Biomaterials* **2011**, *32*, 8730–8742. [CrossRef]
177. Eleraky, N.E.; Allam, A.; Hassan, S.B.; Omar, M.M. Nanomedicine Fight against Antibacterial Resistance: An Overview of the Recent Pharmaceutical Innovations. *Pharmaceutics* **2020**, *12*, 142. [CrossRef] [PubMed]
178. He, B.; Ma, S.; Peng, G.; He, D. TAT-modified self-assembled cationic peptide nanoparticles as an efficient antibacterial agent. *Nanomedicine* **2018**, *14*, 365–372. [CrossRef]
179. Dong, Y.; Zhao, S.; Wang, C.; Liu, W.; Zhang, Y.; Deng, L.; Zhang, J.; Huang, P.; Wang, W.; Dong, A. Combating drug-resistant bacterial infection using biodegradable nanoparticles assembled from comb-like polycarbonates grafted with amphiphilic polyquaternium. *J. Mater. Chem. B* **2021**, *9*, 357–365. [CrossRef]
180. Lam, S.J.; O'Brien-Simpson, N.M.; Pantarat, N.; Sulistio, A.; Wong, E.H.H.; Chen, Y.-Y.; Lenzo, J.C.; Holden, J.A.; Blencowe, A.; Reynolds, E.C.; et al. Combating multidrug-resistant Gram-negative bacteria with structurally nanoengineered antimicrobial peptide polymers. *Nat. Microbiol.* **2016**, *1*, 16162. [CrossRef]
181. Namivandi-Zangeneh, R.; Kwan, R.J.; Nguyen, T.-K.; Yeow, J.; Byrne, F.L.; Oehlers, S.H.; Wong, E.H.H.; Boyer, C. The effects of polymer topology and chain length on the antimicrobial activity and hemocompatibility of amphiphilic ternary copolymers. *Polym. Chem.* **2018**, *9*, 1735–1744. [CrossRef]
182. Zhou, Y.; Zheng, Y.; Wei, T.; Qu, Y.; Wang, Y.; Zhan, W.; Zhang, Y.; Pan, G.; Li, D.; Yu, Q.; et al. Multistimulus Responsive Biointerfaces with Switchable Bioadhesion and Surface Functions. *ACS Appl. Mater. Interfaces* **2020**, *12*, 5447–5455. [CrossRef] [PubMed]
183. Li, W.; Zhang, H.; Li, X.; Yu, H.; Che, C.; Luan, S.; Ren, Y.; Li, S.; Liu, P.; Yu, X.; et al. Multifunctional Antibacterial Materials Comprising Water Dispersible Random Copolymers Containing a Fluorinated Block and Their Application in Catheters. *ACS Appl. Mater. Interfaces* **2020**, *12*, 7617–7630. [CrossRef]
184. Xue, R.; Zhang, X.; Wei, Y.; Zhao, Z.; Liu, H.; Yang, F.; Yin, L.; Song, Z.; Luan, S.; Tang, H. A sulfonate-based polypeptide toward infection-resistant coatings. *Biomater. Sci.* **2021**, *9*, 6425–6433. [CrossRef] [PubMed]
185. Peddinti, B.S.T.; Scholle, F.; Vargas, M.G.; Smith, S.D.; Ghiladi, R.A.; Spontak, R.J. Inherently self-sterilizing charged multiblock polymers that kill drug-resistant microbes in minutes. *Mater. Horiz.* **2019**, *6*, 2056–2062. [CrossRef]
186. Muralidharan, S.K.; Bauman, L.; Anderson, W.A.; Zhao, B. Recyclable antimicrobial sulphonated poly (ether ether ketone)—Copper films: Flat vs. micro-pillared surfaces. *Mater. Today Commun.* **2020**, *25*, 101485. [CrossRef]
187. Zhu, S.; Xue, R.; Yu, Z.; Zhang, X.; Luan, S.; Tang, H. Transition of Conformation and Solubility in β-Sheet-Structured Poly(l-cysteine)s with Methylthio or Sulfonium Pendants. *Biomacromolecules* **2021**, *22*, 1211–1219. [CrossRef] [PubMed]
188. Chouirfa, H.; Evans, M.D.M.; Bean, P.; Saleh-Mghir, A.; Crémieux, A.C.; Castner, D.G.; Falentin-Daudré, C.; Migonney, V. Grafting of Bioactive Polymers with Various Architectures: A Versatile Tool for Preparing Antibacterial Infection and Biocompatible Surfaces. *ACS Appl. Mater. Interfaces* **2018**, *10*, 1480–1491. [CrossRef]
189. Sciuto, E.L.; Filice, S.; Coniglio, M.A.; Faro, G.; Gradon, L.; Galati, C.; Spinella, N.; Libertino, S.; Scalese, S. Antimicrobial s-PBC Coatings for Innovative Multifunctional Water Filters. *Molecules* **2020**, *25*, 5196. [CrossRef]
190. Hasan, J.; Crawford, R.J.; Ivanova, E.P. Antibacterial surfaces: The quest for a new generation of biomaterials. *Trends Biotechnol.* **2013**, *31*, 295–304. [CrossRef]
191. Kelleher, S.M.; Habimana, O.; Lawler, J.; O'Reilly, B.; Daniels, S.; Casey, E.; Cowley, A. Cicada Wing Surface Topography: An Investigation into the Bactericidal Properties of Nanostructural Features. *ACS Appl. Mater. Interfaces* **2016**, *8*, 14966–14974. [CrossRef]
192. Pogodin, S.; Hasan, J.; Baulin, V.A.; Webb, H.K.; Truong, V.K.; Phong Nguyen, T.H.; Boshkovikj, V.; Fluke, C.J.; Watson, G.S.; Watson, J.A.; et al. Biophysical model of bacterial cell interactions with nanopatterned cicada wing surfaces. *Biophys. J.* **2013**, *104*, 835–840. [CrossRef]
193. Ivanova, E.P.; Linklater, D.P.; Werner, M.; Baulin, V.A.; Xu, X.; Vrancken, N.; Rubanov, S.; Hanssen, E.; Wandiyanto, J.; Truong, V.K.; et al. The multi-faceted mechano-bactericidal mechanism of nanostructured surfaces. *Proc. Natl. Acad. Sci. USA* **2020**, *117*, 12598–12605. [CrossRef]
194. Truong, V.K.; Geeganagamage, N.M.; Baulin, V.A.; Vongsvivut, J.; Tobin, M.J.; Luque, P.; Crawford, R.J.; Ivanova, E.P. The susceptibility of *Staphylococcus aureus* CIP 65.8 and *Pseudomonas aeruginosa* ATCC 9721 cells to the bactericidal action of nanostructured *Calopteryx haemorrhoidalis* damselfly wing surfaces. *Appl. Microbiol. Biotechnol.* **2017**, *101*, 4683–4690. [CrossRef]
195. Michalska, M.; Gambacorta, F.; Divan, R.; Aranson, I.S.; Sokolov, A.; Noirot, P.; Laible, P.D. Tuning antimicrobial properties of biomimetic nanopatterned surfaces. *Nanoscale* **2018**, *10*, 6639–6650. [CrossRef]
196. Modaresifar, K.; Kunkels, L.B.; Ganjian, M.; Tümer, N.; Hagen, C.W.; Otten, L.G.; Hagedoorn, P.-L.; Angeloni, L.; Ghatkesar, M.K.; Fratila-Apachitei, L.E.; et al. Deciphering the Roles of Interspace and Controlled Disorder in the Bactericidal Properties of Nanopatterns against *Staphylococcus aureus*. *Nanomaterials* **2020**, *10*, 347. [CrossRef]
197. Linklater, D.P.; de Volder, M.; Baulin, V.A.; Werner, M.; Jessl, S.; Golozar, M.; Maggini, L.; Rubanov, S.; Hanssen, E.; Juodkazis, S.; et al. High Aspect Ratio Nanostructures Kill Bacteria via Storage and Release of Mechanical Energy. *ACS Nano* **2018**, *12*, 6657–6667. [CrossRef]
198. Wang, X.; Lyu, C.; Wu, S.; Ben, Y.; Li, X.; Ge, Z.; Zou, H.; Tian, D.; Yu, Y.; Ding, K. Electrophoresis-Deposited Mesoporous Graphitic Carbon Nitride Surfaces with Efficient Bactericidal Properties. *ACS Appl. Bio Mater.* **2020**, *3*, 2255–2262. [CrossRef]

199. Chen, J.; Peng, H.; Wang, X.; Shao, F.; Yuan, Z.; Han, H. Graphene oxide exhibits broad-spectrum antimicrobial activity against bacterial phytopathogens and fungal conidia by intertwining and membrane perturbation. *Nanoscale* **2014**, *6*, 1879–1889. [CrossRef]
200. Luo, Y.; Ge, M.; Lin, H.; He, R.; Yuan, X.; Yang, C.; Wang, W.; Zhang, X. Anti-Infective Application of Graphene-Like Silicon Nanosheets via Membrane Destruction. *Adv. Healthc. Mater.* **2020**, *9*, e1901375. [CrossRef]
201. Sun, W.; Wu, F.-G. Two-Dimensional Materials for Antimicrobial Applications: Graphene Materials and beyond. *Chem. Asian J.* **2018**, *13*, 3378–3410. [CrossRef] [PubMed]
202. Shi, T.; Hou, X.; Guo, S.; Zhang, L.; Wei, C.; Peng, T.; Hu, X. Nanohole-boosted electron transport between nanomaterials and bacteria as a concept for nano-bio interactions. *Nat. Commun.* **2021**, *12*, 493. [CrossRef]
203. Ricciardi, B.F.; Muthukrishnan, G.; Masters, E.; Ninomiya, M.; Lee, C.C.; Schwarz, E.M. *Staphylococcus aureus* Evasion of Host Immunity in the Setting of Prosthetic Joint Infection: Biofilm and Beyond. *Curr. Rev. Musculoskelet. Med.* **2018**, *11*, 389–400. [CrossRef]
204. Wu, Y.-K.; Cheng, N.-C.; Cheng, C.-M. Biofilms in Chronic Wounds: Pathogenesis and Diagnosis. *Trends Biotechnol.* **2019**, *37*, 505–517. [CrossRef]
205. Yamada, K.J.; Kielian, T. Biofilm-Leukocyte Cross-Talk: Impact on Immune Polarization and Immunometabolism. *J. Innate Immun.* **2019**, *11*, 280–288. [CrossRef]
206. Guo, G.; Zhang, H.; Shen, H.; Zhu, C.; He, R.; Tang, J.; Wang, Y.; Jiang, X.; Wang, J.; Bu, W.; et al. Space-Selective Chemodynamic Therapy of $CuFe_5O_8$ Nanocubes for Implant-Related Infections. *ACS Nano* **2020**, *14*, 13391–13405. [CrossRef]
207. Mittler, R. ROS Are Good. *Trends Plant Sci.* **2017**, *22*, 11–19. [CrossRef]
208. Zhang, C.; Bu, W.; Ni, D.; Zhang, S.; Li, Q.; Yao, Z.; Zhang, J.; Yao, H.; Wang, Z.; Shi, J. Synthesis of Iron Nanometallic Glasses and Their Application in Cancer Therapy by a Localized Fenton Reaction. *Angew. Chem. Int. Ed Engl.* **2016**, *55*, 2101–2106. [CrossRef]
209. Mocan, T.; Matea, C.T.; Pop, T.; Mosteanu, O.; Buzoianu, A.D.; Suciu, S.; Puia, C.; Zdrehus, C.; Iancu, C.; Mocan, L. Carbon nanotubes as anti-bacterial agents. *Cell. Mol. Life Sci.* **2017**, *74*, 3467–3479. [CrossRef]
210. González-Lavado, E.; Valdivia, L.; García-Castaño, A.; González, F.; Pesquera, C.; Valiente, R.; Fanarraga, M.L. Multi-walled carbon nanotubes complement the anti-tumoral effect of 5-Fluorouracil. *Oncotarget* **2019**, *10*, 2022–2029. [CrossRef]
211. Seo, Y.; Hwang, J.; Kim, J.; Jeong, Y.; Hwang, M.P.; Choi, J. Antibacterial activity and cytotoxicity of multi-walled carbon nanotubes decorated with silver nanoparticles. *Int. J. Nanomed.* **2014**, *9*, 4621–4629. [CrossRef]
212. David, M.E.; Ion, R.-M.; Grigorescu, R.M.; Iancu, L.; Holban, A.M.; Nicoara, A.I.; Alexandrescu, E.; Somoghi, R.; Ganciarov, M.; Vasilievici, G.; et al. Hybrid Materials Based on Multi-Walled Carbon Nanotubes and Nanoparticles with Antimicrobial Properties. *Nanomaterials* **2021**, *11*, 1415. [CrossRef]